

A general algorithm for the optimization of photovoltaic modules layout on irregular rooftop shapes

A. Barbón^a, M. Ghodbane^b, L. Bayón^{c,*}, Z. Said^{d,e}

^a Department of Electrical Engineering, University of Oviedo, Spain

^b Department of Mechanical Engineering, Saad Dahlab University of Blida 1, Algeria

^c Department of Mathematics, University of Oviedo, Spain

^d Department of Sustainable and Renewable Energy Engineering, University of Sharjah, United Arab Emirates

^e U.S.-Pakistan Center for Advanced Studies in Energy (USPCAS-E), National University of Sciences and Technology (NUST), Pakistan

ARTICLE INFO

Handling Editor: Jiri Jaromir Klemeš

Keywords:

Photovoltaics modules
Irregular rooftop shapes
Optimal distribution
Maximum energy
Self-shading of photovoltaic modules

ABSTRACT

Although the installation of photovoltaic systems on roofs is a successful investment, rooftop space availability has been identified as a significant limiting factor in achieving zero-energy buildings, especially by building components such as chimneys, elevator machine rooms, fans, plumbing vents, etc. This study presents a general algorithm for the optimal deployment of photovoltaic module rows installed on irregular flat roof shapes. The presented algorithm takes into account the irregular rooftop shape, the self-shading of photovoltaic modules, the inclusion of building components, commercial photovoltaic modules with different sizes, mounting systems with different configurations, distances required for maintenance, and the technical reports to minimize shading effects. The proposed algorithm allowed to increase in the amount of solar energy received by the photovoltaic modules. The optimization process takes into account the weather conditions at the specific location. The optimization algorithm was implemented using a specific Mathematica™ code in which the commands used in the development of the code were introduced to facilitate its replication. The optimization algorithm output provides the essential parameters for the optimal photovoltaic system design such as: the optimum number of mounting systems and their configuration, the optimum tilt angle of the mounting system and its dimensions, the photovoltaic module model, the maximum total area of the photovoltaic field and the maximum annual energy captured by the photovoltaic modules. We compared the mounting system layout obtained with the proposed algorithm with the tilt angle photovoltaic module layout recommended by three technical papers (*IDAIE Technical Report*, Lorenzo's equation and Jacobson's equation) with respect to photovoltaic field area gain, energy gain and levelized cost of energy. The optimal photovoltaic module layout obtains the maximum photovoltaic field area gain of 35.52% with respect to the Jacobson's equation and the minimum of 32.29% with respect to the *IDAIE Technical Report*. The optimal photovoltaic module layout obtains the maximum energy gain of 27.83% with respect to the Jacobson's equation and the minimum of 24.84% with respect to the *IDAIE Technical Report*. The levelized cost of energy of the optimal *PV* module layout is lower than that of the other arrangements studied. The algorithm presented may be useful for decision-makers or policymakers in determining the optimal distribution of photovoltaic modules on irregular rooftop shapes.

1. Introduction

Given the increasing global demand for energy, the exploitation of various renewable sources is the best solution to confront global energy crises, as solar energy enjoys the greatest acceptance and exploitation compared to the rest of the other renewable energy sources (wind energy, geothermal energy, biomass energy, and hydropower). Therefore, Solar energy is the most important source of renewable energies and

can be exploited to generate electricity thermally in concentrating solar power plants (*CSP*) (Ghodbane et al., 2019) or by using photovoltaic (*PV*) system. Regarding *CSP* plants, they use various types of solar concentrators (Ghodbane et al., 2019), as its initial investment cost is high (Said et al., 2022) and has the advantage that it can be combined with thermal energy storage. Regarding *PV* technology, is less costly

* Corresponding author.

E-mail addresses: barbon@uniovi.es (A. Barbón), ghodbane@uniovi.es (M. Ghodbane), bayon@uniovi.es (L. Bayón), zsaid@sharjah.ac.ae (Z. Said).

<https://doi.org/10.1016/j.jclepro.2022.132774>

Received 27 April 2022; Received in revised form 2 June 2022; Accepted 17 June 2022

Available online 21 June 2022

0959-6526/© 2022 Elsevier Ltd. All rights reserved.

and can generate electricity on a small scale. Therefore, *PV* systems are considered a viable technological solution to help reduce dependence on fossil fuels, as its potential is demonstrated by the exponential increase in installed capacity worldwide, where the cumulative solar photovoltaic power generation capacity from 23 *GW* in 2009 to 754 *GW* in 2020 (British Petroleum, 2021). According to Jacobson et al. (2017), the electricity generated by photovoltaic systems in 2050 will be distributed as follows 21.40% in *PV* plants, 14.90% in residential rooftop *PV*, and 11.60% in commercial/government rooftops, knowing that this study has been supported by the International Energy Agency report (IEA, 2019), which indicates that the main driver for the development of rooftop *PV* systems was the owners' investments, and this development is the result of four main factors, knowing that the choice of installing *PV* modules on the roof depends not only on the amount of solar irradiance received in a particular location, but also on the following factors (Lang et al., 2015):

- (i) Strong reduction in the cost of photovoltaic systems, where the Levelized Cost of Energy (*LCOE*) can be used to measure a *PV* system's economic efficiency. According to the International Renewable Energy Agency (IRENA, 2019), the weighted average *LCOE* is expected to be between 0.02 and 0.08 USD/kWh in 2030, and between 0.014 and 0.05 USD/kWh in 2050;
- (ii) Electricity retail prices, where the electricity sales prices to homeowners are higher than electricity market prices due to taxes and transmission and distribution (Gernaat et al., 2020);
- (iii) Net metering policy, where this instrument allows homeowners to sell excess electricity to the grid at a retail price (Iliopoulos et al., 2020);
- (iv) Subsidy benefit, where this instrument provides homeowners with direct financial incentives that reduce the cost of adopting photovoltaic technology (Tibebu et al., 2021).

In addition, Gernaat et al. estimated that 31.86% of the global rooftop area will potentially be suitable for rooftop *PV* systems, that is equivalent to an area of 36 billion m^2 (Gernaat et al., 2020). Moreover, the total residential rooftop area in the European Union amounts to around 19 billion m^2 (Odyssee-Mure, 2015). The rooftops of buildings are also the best place to install small-scale photovoltaic systems (Dehwah et al., 2018). In this regard, the study of the potential of installing photovoltaic systems on rooftops has been the focus of many researchers as (Jurasz et al., 2020; Lau et al., 2021), knowing that the maximum installed capacity of *PV* modules on horizontal rooftops depends on the following parameters related to the *PV* modules: tilt angle of the *PV* modules, the orientation of the *PV* modules, the distance between the *PV* modules rows, the number of *PV* modules, and dimensions of the *PV* modules. When interacting these parameters with rooftop parameters, such as available rooftop surface, building components, rooftop shape, and rooftop orientation, the complexity of the *PV* system design increases significantly.

In addition, several problems are often encountered during the design of the *PV* modules deployment on buildings' rooftops:

- (i) Available rooftop area, where the restricted space availability of rooftops has been identified as a major limiting factor in achieving zero-energy buildings (Giffith et al., 2006). Several authors have developed methods for estimating available rooftop areas, the most important of which are (Melius et al., 2013): constant-value Methods, manual selection methods, and *GIS*-based methods. The first method is easy to compute, but the results are challenging to validate. The second method is computationally time-consuming and not easily replicable in several regions. The third method can be replicated in several regions and require a lot of computer resources;

- (ii) Building components, where several building components restrict the viability of rooftop *PV*, such as chimneys, elevator machine rooms, fans, plumbing vents, etc. Concerning this aspect, several works take into account the shading losses due to building components (Siraki and Pillay, 2012), however, they ignore the self-shading losses of *PV* modules. In addition, other studies such as Bayón-Cueli et al. (2021) and Barbón et al. (2022) do not consider building components;
- (iii) Rooftop shape, which plays a crucial role in *PV* systems installation, where the basic shapes of a rooftop are rectangular and L-shaped (Hachem et al., 2011). Consequently, several studies have focused on investigating the optimal distribution of *PV* modules on different basic shapes of rooftops, where Bayón et al. presented the optimal distribution of *PV* modules on rectangular rooftop shapes (Bayón-Cueli et al., 2021). In addition, Barbón et al. (2022) determined the optimal distribution of *PV* modules on simple shapes of rooftops. Likewise, Ioannou et al. presented the optimal configuration of the *PV* module rows when these are installed on a square rooftop shape (Ioannou et al., 2014), where they did not take into account the irregular rooftop shapes. Variants of the L-shape are characterized by the use of several additional angles, increasing the complexity of the problem considerably. Also, Hachem et al. presented a detailed study of the L-shape variants (Hachem et al., 2011). According to Dehwah et al. (2018), the irregular rooftop geometry of some buildings is a further limitation to their use for photovoltaic systems. Therefore, this work aims to determine the optimal distribution of *PV* modules on irregular rooftop shapes;
- (iv) Self-shading of *PV* modules, where it reduces the incident solar irradiance on *PV* modules on specific modules caused by nearby rows of *PV* modules. It is almost impossible to avoid these energy losses, although they can be minimized. Due to its importance, these shading losses are regulated by several legislations (IDAE, 2011). However, several studies that determine the optimum tilt angle and orientation of *PV* modules do not take these losses into account (Al Garmi et al., 2019; Jafarkazemi and Saadabadi, 2013). Also, Bayón-Cueli et al. (2021) disregarded the effect of shading in total incident energy calculations (Bayón-Cueli et al., 2021). In Barbón et al. (2022) only the energy generated during the operating hours without shading was taken into account. For this purpose, the solar irradiance incident on the *PV* modules was determined by the product between the adjusted solar irradiation curve as a function of the tilt angle $\mathbb{H}_i(\beta)$ and the total area of *PV* modules $A_{PV}^T(\beta)$;
- (v) The high number of commercial photovoltaic modules with different sizes. *PV* modules come in a wide range of sizes, depending on the manufacturer. On average, residential *PV* modules contain 60 solar cells, and commercial *PV* modules are slightly larger, usually containing 72 solar cells (IEA, 2019). The size of the module has been continuously increased (IEA, 2019). Therefore, the number of *PV* module combinations for a given installation is very high, complicating the optimal solution to the problem. Only one *PV* module size is used in the study presented by Barbón et al. (2022). And most studies do not take into account the size of the *PV* module (Al Garmi et al., 2019; Jafarkazemi and Saadabadi, 2013);
- (vi) *PV* module mounting system, where this system allows *PV* modules to be securely attached to the ground. However, the mounting system can be fixed or tracked. In the building sector, solar tracking systems are not cost-effective (Mousazadeh et al., 2009). Therefore, in this study, the mounting system used is fixed. The configurations of this type of mounting system play a key role in optimizing the distribution of *PV* modules on the rooftop and complicates its optimal solution. Several studies take into account the configuration of the mounting system in their work (Bayón-Cueli et al., 2021; Barbón et al., 2022), but most studies do not consider this parameter (Wang et al., 2018; Korsavi et al., 2018).

It can be concluded that the design of rooftop *PV* systems is a very complex process that involves many interrelated parameters. Therefore, the design of an algorithm to facilitate this task is necessary. Thus, the objective of the present work is to provide a methodology that allows the optimal distribution of *PV* modules when these are installed on irregular flat rooftop shapes. The optimization process is performed by considering the parameters related to the *PV* modules (tilt angle and orientation of the *PV* modules, distance between the *PV* modules rows, number of *PV* modules, dimensions of the *PV* modules, and mounting system configuration) and the constraints and limitations of the rooftop (available rooftop surface, building components, rooftop shape, and rooftop orientation). The proposed algorithm uses well-established methods for the estimation of solar irradiance received on the tilted plane (Barbón et al., 2020) and incorporates a numerical model which calculates the self-shading energy losses of *PV* modules and the shading energy losses due to building components. This algorithm was applied to the case of Almería (Spain). Still, it can be used worldwide as the method used to determine solar irradiance (Barbón et al., 2020) is designed for this purpose (Barbón et al., 2021). In addition, it interacts with the determination of the self-shading losses of *PV* modules and the shading losses due to building components. The distribution of *PV* rows on irregular flat rooftop shapes is formulated as a two-dimensional rectangle packing problem. Heuristic techniques were used to design practical algorithms for this problem.

As mentioned above, several studies analyzed the design of the *PV* modules deployment on rooftops, but such studies had the following limitations:

- (i) Several studies were conducted to optimize the distribution of *PV* modules on basic shapes of rooftops, and there was still a lack of study using irregular rooftop shapes;
- (ii) Self-shading of *PV* modules causes high-energy losses, but many studies do not take this into account;
- (iii) Several building components restrict the viability of rooftop *PV*, but some previous studies did not consider this fact in their approach;
- (iv) Although a large number of commercial *PV* module sizes complicates the optimal solution to the problem, most studies do not take them into account, or only one size is considered;
- (v) Most studies do not consider the mounting system, so the results will deviate substantially from reality.

The specific contributions of this study can be summarized in the following proposals:

- (i) A methodology to maximize the amount of energy absorbed by an irregular rooftop shapes.
- (ii) For each tilt angle, the algorithm maximizes the total energy of the *PV* modules on the rooftop, taking into account the self-shading of the *PV* modules and the building components.
- (iii) The study considers the size of commercial *PV* modules and mounting systems as inputs.

Therefore, the present work addresses a gap in the scientific literature, as it aims to include in the proposed algorithm all the limitations raised in previous studies. In another meaning, this is the first study that considers all the limitations mentioned above.

A multi-condition analysis without computational constraints is necessary to meet all the constraints posed in the problem. Mathematica™ software has been chosen for, among other reasons, the simplicity of the theoretical formulation and the high performance. Extensive Mathematica™ code is developed to establish the proposed constraints and efficiently solve the problem of optimizing the arrangement of *PV* modules on irregular flat rooftop shapes.

The developed algorithm can enable engineers, architects, construction managers, owners, etc., to determine the optimal distribution of *PV* modules on irregular flat rooftop shapes. The application of the

optimization algorithm results in the optimal number of mounting systems and their configuration, the tilt angle and dimensions of each mounting system, the model of the photovoltaic module, the maximum total photovoltaic modules area, and the maximum annual incident energy on the photovoltaic modules.

This paper is organized with the following structure: The problem approach with the constraints posed is presented in Section 2. The optimization formulation is outlined in Section 3. The valuation indicators are provided in Section 4. The methodology application and the analysis of the results are presented in Section 5. Finally, Section 6 summarizes the main contributions and the conclusions of the paper.

2. Problem approach

This engineering problem is contextualized within the framework of the relevant European legislation and the high electricity consumption in the building sector. In 2019, almost 55% of global electricity consumption was consumed in building operations (UN, 2020). Therefore, electrification through renewable sources (e.g., *PV* systems) in the building sector is essential to comply with the Paris Agreement (UN, 2015). Several European directives require new buildings to obtain part of their energy needs from renewable sources. One of them is the Directive 2009/28/EC (EU, 2009). A policy framework for climate and energy for the period 2020–2030 has been established by the European Commission (EU, 2014). EU directives, in particular Directive 2018/2001/EC (EU, 2018), have also addressed the requirements for the use of renewable energy in new and renovated buildings.

The study deals with the optimal distribution of *PV* modules on flat rooftops under the following conditions: (i) irregular rooftop shapes; (ii) self-shading of *PV* modules; (iii) inclusion of building components; (iv) commercial *PV* modules with different sizes; and (v) mounting systems with different configurations. These aspects are not sufficiently addressed in the literature. Therefore, when such a high number of parameters need to be considered, it can be difficult for experts to optimize the choice of *PV* system components for a given location.

2.1. Irregular rooftop shape and building components

A general irregular flat rooftop shape is considered in this study. The rectangular and *L* shapes can be considered as the basic regular shapes (Hachem et al., 2011). Irregular shapes can be derived from the variation of these shapes. Hachem et al. defined the *L* shape as the composition of the main wing and an attached branch (Hachem et al., 2011). *L* shape variants and therefore irregular shapes are characterized by angles deviating from 90° of the angle between the wings of the *L* shape. During the study as shown in Fig. 1, the shape of the irregular roof was taken into account, as this roof was chosen because it covers two conditions from the study, the shape of the irregular roof facing south and the building components, where \bar{P} is the available roof area. Regarding the proposed algorithm, it can optimize any other type of regular or irregular rooftop shape.

The work employs *GIS* (Geographical Information System) techniques to determine the building rooftop's Universal Transverse Mercator (*UTM*) coordinates. Specifically, the software used is the *QGIS*™, because it is free software with an open code (Sebbah et al., 2021; Park et al., 2019). Moreover, the National Geographic Information Center of the Government of Spain provides a database on Landsat image (NGIC, 2022).

A subproblem whose solution is necessary to implement the proposed algorithm is to obtain the *UTM* coordinates in the Mathematica™ software. For this purpose and as shown in Eq. (1), the user will select the most adequate number of points $p[i], i = 1, 2, \dots, n$, in the Mathematica™ software for each particular case to form a polygon that adapts itself with sufficient precision to the limits of the irregular rooftop shape.

$$P = \text{Polygon}[\text{Table}[p[i], \{i, 1, n\}]] \quad (1)$$

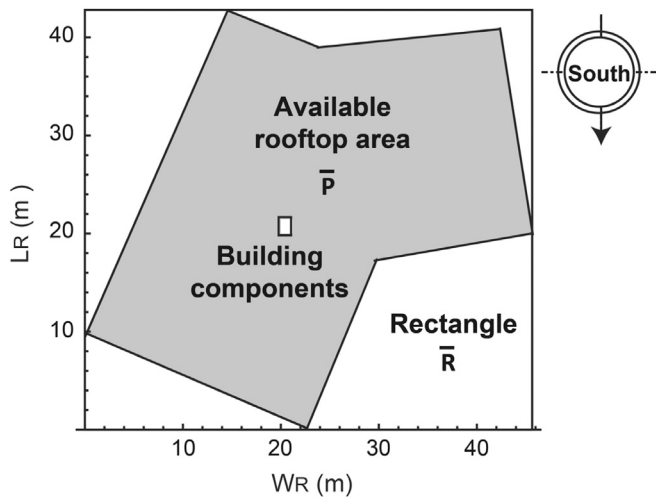


Fig. 1. Irregular rooftop shape under study.

As shown in Fig. 1, the projection P is obtained, and it can be inscribed in a rectangle R with dimensions $W_R \times L_R$, where, for convenience, the lower-left point of R is taken as the origin O :

$$R = \text{BoundingRegion}[\{\text{Table}[p[i], \{i, 1, n\}]\}, \text{“MinRectangle”}] \quad (2)$$

$$\bar{R} = \text{TransformedRegion}[R, \text{TranslationTransform}[-O]] \quad (3)$$

$$\bar{P} = \text{TransformedRegion}[P, \text{TranslationTransform}[-O]] \quad (4)$$

2.2. Photovoltaic field geometry

The PV field is horizontal and consists of a number (N_{MS}) of PV module mounting systems with a longitudinal installation distance (e_l) between them. Each mounting system is inclined with a tilt angle (β) for the horizontal and azimuth angle (γ). The azimuth angle (γ) of the mounting system (as the majority of the authors consider Chinchilla et al., 2021) will be zero degree in the Northern hemisphere, while the tilt angle (β) of the mounting system will be optimized, i.e., the tilt angle (β) will be an algorithm output. The commercial mounting system has length (L) and width (W). The commercial PV module has a length (L_{PV}) and width (W_{PV}). Clamps are used to fix the PV modules to the mounting systems. Therefore, a transversal installation distance (e_t) between PV modules has been considered.

In a Field and as shown in Fig. 2a, which shows a row of PV modules with a south orientation (i.e., $\gamma = 0^\circ$), to determine the effect of self-shading, other parameters are required, the most important of which is the longitudinal incidence angle θ_l .

$$\tan \theta_l = \frac{\cos \gamma_s}{\tan \alpha_s} = \tan \theta_z \cos \gamma_s \quad (5)$$

where α_s in ($^\circ$) is the height angle of the sun, θ_z in ($^\circ$) is the zenith angle of the sun, and γ_s in ($^\circ$) is the azimuth of the sun. Fig. 2.b shows the design parameters.

According to Barbón et al. (2022), the configuration of the mounting system is determined based on two parameters, X and Y . As for the parameter X , it represents the number of the vertical consecutive PV modules in each row. This parameter can take the values 1, 2, 3, etc., although, for urban applications, its value usually 1 or 2, as regulations typically limit the height that PV systems placed on rooftops can reach. Regarding the parameter Y , it can take the letter V or H , where the letter V (H) refers to the mounting system configuration in which the PV module length (PV module width) is the reference for the tilt angle. Examples of this nomenclature are $1V$, $2H$, etc. Fig. 3b shows the $2V$ mounting system configuration ($W = W_{PV}$, $L = 2L_{PV}$), but other configurations may be the optimal solution to the problem, e.g., $1V$

configuration, $2H$ configuration (see Fig. 3(a-d)). This parameter will be an algorithm output.

The selection of the dimensions of the PV modules depends on the size and shape of the rooftop surface. This selection is not without difficulty due to the many commercially available PV modules on the PV market, where Belsky et al. presented a study of the technical characteristics of 1300 PV modules from multiple manufacturers in the range from 100 to 450 (W) (Belsky et al., 2022). This work covers most commercial PV modules as of the first half of 2021, where this work will be a reference point for our study, given that the commercial PV module will be the output of an algorithm.

2.3. Solar irradiance on tilted plane

The latitude of the rooftop location affects the optimum deployment of the PV modules, and in order to use the proposed algorithm at different latitudes, a suitable solar irradiance model is needed. Since the readily available data for many locations are the monthly solar irradiance values on horizontal surfaces, whether beam or diffuse, and their sum being the total solar irradiance, the solar irradiance model used will be as input to the studied algorithm considering the effect of crossing clouds on the used solar irradiance model.

In this study, the method proposed by Barbón et al. (2020) was adopted to calculate the adjusted hourly solar irradiance (beam and diffuse) on a horizontal surface, taking into account all weather conditions in the locations selected for this study. Since this method involves the use of meteorological conditions for each site chosen to study, it gives good results and has been used in many studies, including Bayón-Cueli et al. (2021), Barbón et al. (2022) and Jallal et al. (2020).

Eq. (6) has been used to determine the solar irradiance on a tilted surface (Duffie and Beckman, 2013):

$$\begin{aligned} \mathbb{I}_t(n, \beta, T) = & \mathbb{I}_{bh}(n, T) \cdot \frac{\cos \theta_i}{\cos \theta_z} + \mathbb{I}_{dh}(n, T) \cdot \left(\frac{1 + \cos \beta}{2} \right) \\ & + (\mathbb{I}_{bh}(n, T) + \mathbb{I}_{dh}(n, T)) \cdot \rho_g \cdot \left(\frac{1 - \cos \beta}{2} \right) \end{aligned} \quad (6)$$

Regarding \mathbb{I}_{bh} in (W/m^2) and \mathbb{I}_{dh} in (W/m^2), they are the amount of adjusted solar irradiance (beam and diffuse, respectively) according to Barbón et al. (2020). The rest of the parameters are as follows: n it is a day of year (regular or leap year); it changes from 1 to 365 in a normal year, and to 366 in a leap year, since each date of the year has a specific (n) number. β in ($^\circ$) is the tilt angle, θ_z in ($^\circ$) is the zenith angle of the sun, θ_i in ($^\circ$) is the incidence angle calculated according to Duffie and Beckman (2013), ρ_g (dimensionless) is the ground reflectance, and T in (h) is the solar time. In addition, the isotropic model of Liu and Jordan is used to determine the diffuse, and the ground reflected solar irradiance on a tilted surface (Liu and Jordan, 1963), as many recent works have used this model, most notably (Makhdoomi and Askarzadeh, 2021; Mamun et al., 2021; Conceição et al., 2019).

3. Optimization formulation

To find the optimal distribution of PV modules on flat rooftops of different latitudes, a methodology has been proposed with a flowchart as shown in Fig. 4.

The presented methodology follows these steps:

- (i) Maximization the total area of the PV modules $A_{PV}^T(\beta)$;
- (ii) Determination of operating periods of a PV system;
- (iii) Calculation of the effective area of PV modules $A_{PV}^E(n, \beta, T)$;
- (iv) Maximization of effective annual energy incident on PV modules $E_a(\beta)$.

The optimization algorithm has been implemented with specific Mathematica™ code, and in order to facilitate its replication, the commands used in the development of the code have been introduced.

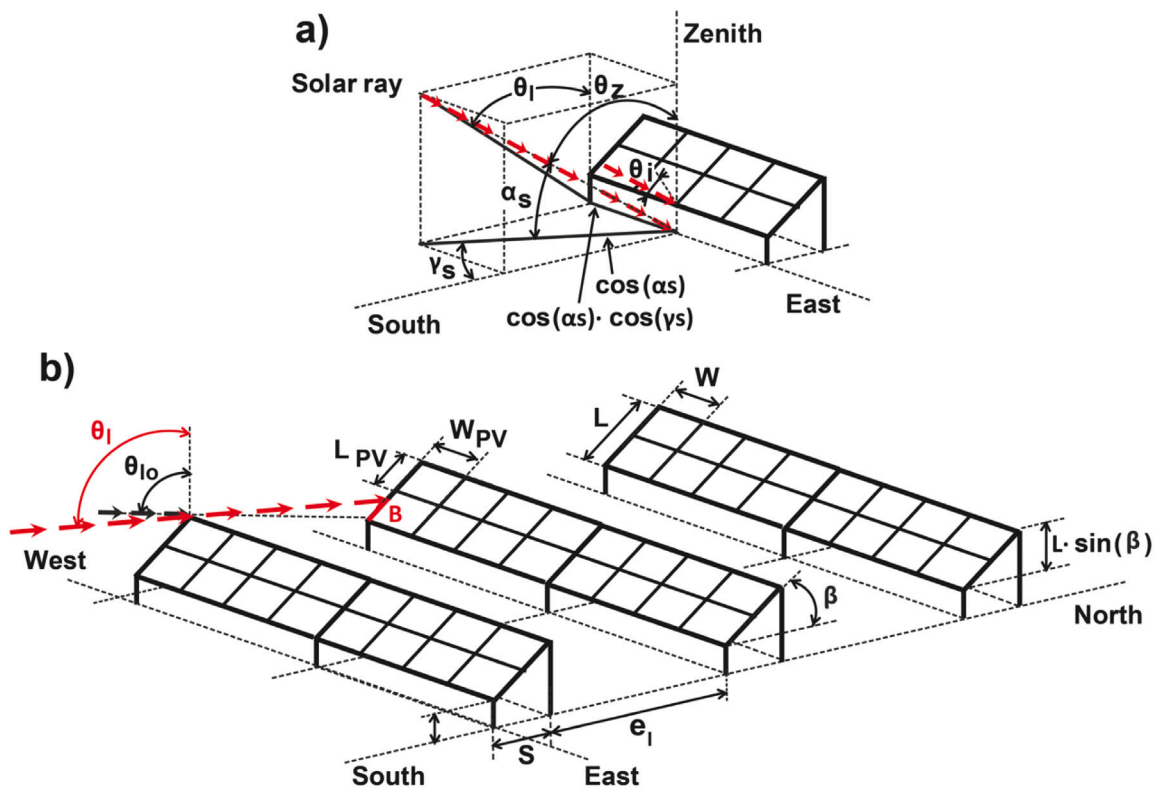


Fig. 2. Photovoltaic field geometry: (a) a row of south-orientated PV modules, (b) design parameters.

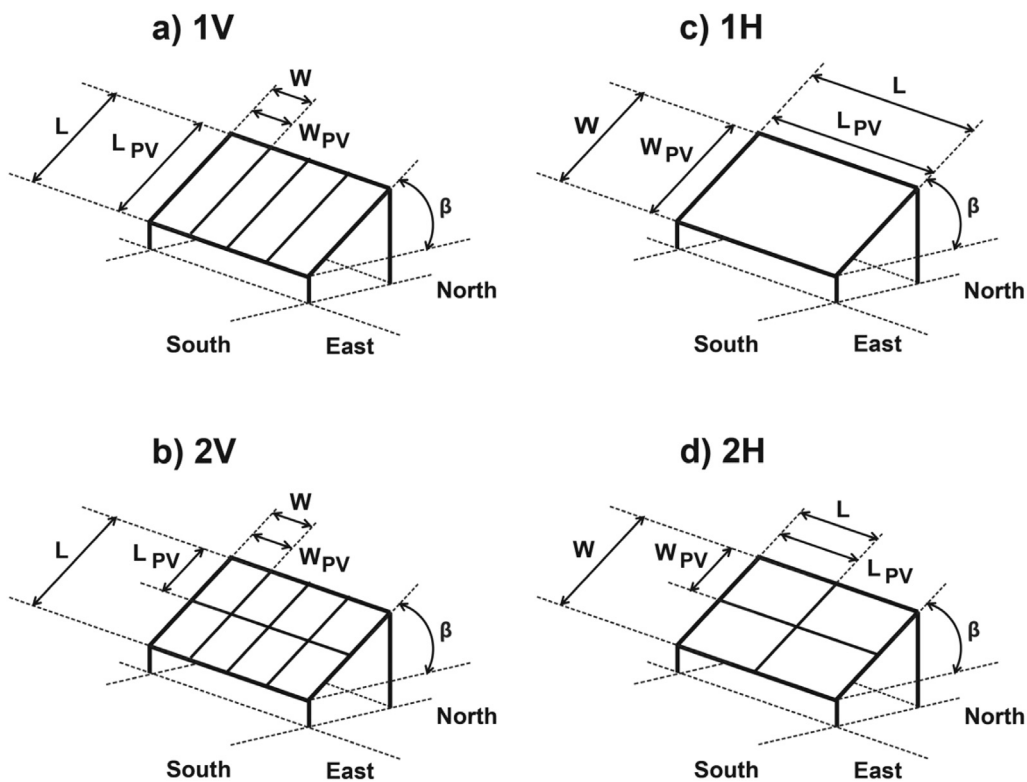


Fig. 3. Some possibilities of mounting system configurations.

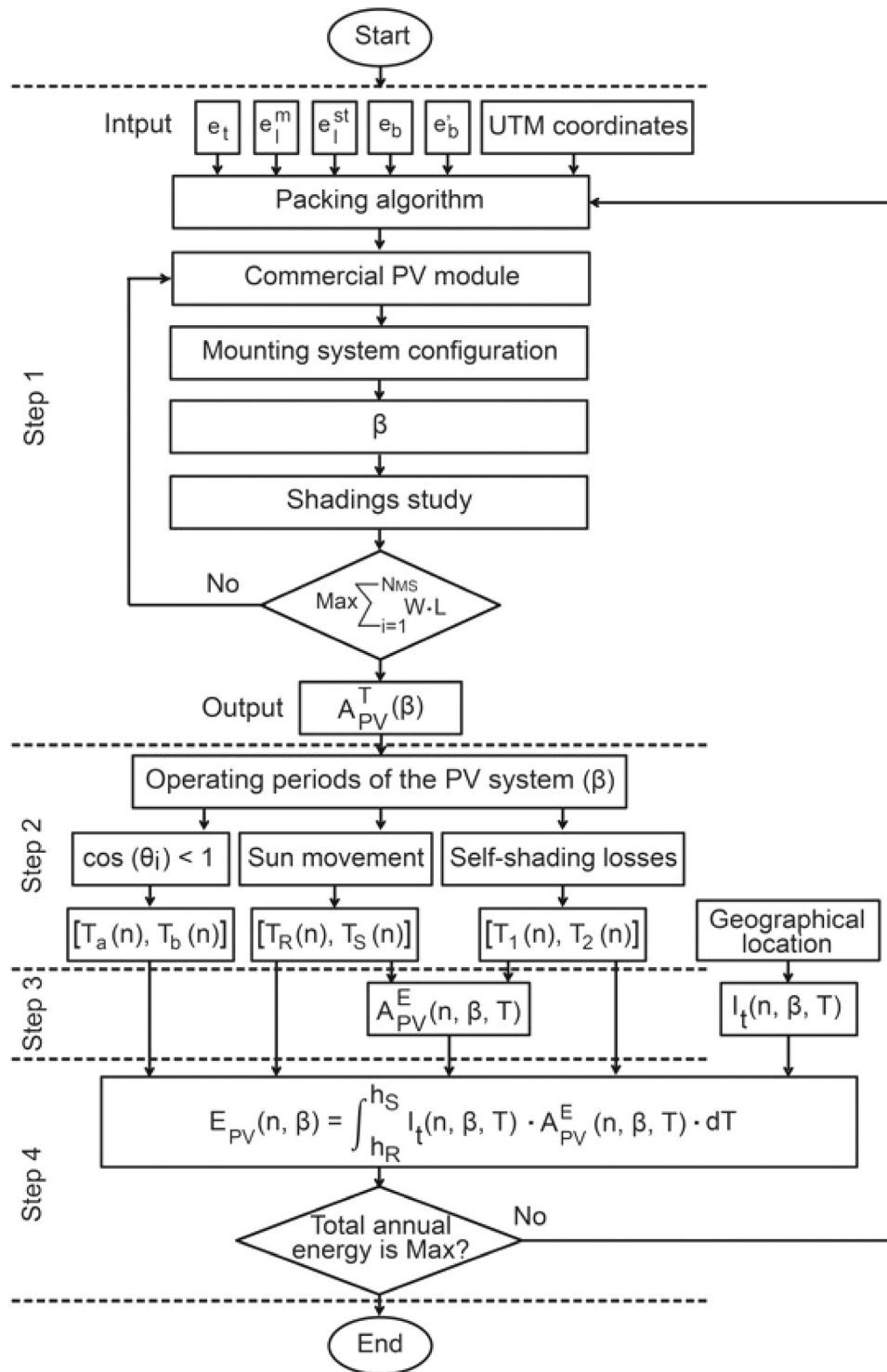


Fig. 4. Flowchart of the algorithm.

3.1. Maximization of total PV modules area

The problem of this first step of the methodology is to find an optimal way to distribute the PV modules on building rooftops. The proposed solution based on the packing problem is one of the best ways to solve this problem. Various forms of packing problems related to the deployment of solar technologies on building rooftops have been studied in the literature.

The distribution of PV modules on roofs was also studied using packing algorithms, as rectangular roofs without building components

were discussed by Bayón-Cueli et al. (2021), and simple shapes for roofs without building components were studied by Barbón et al. (2022). However, none of them faces the same constraints as those presented in this paper, where these restrictions significantly increase the complexity of the currently studied problem.

Among the packing algorithms, strip-packing problem, area minimization problem, two-dimensional bin packing problem, two-dimensional knapsack problem, two-dimensional cutting stock problem, pallet loading problem, etc., proposed in the literature (Imahori

et al., 2006), to solve this packing problem, the special type of two-dimensional rectangle packing problem has been chosen. Therefore, Eq. (7) shows the total area of PV mounting systems that need to be maximized.

$$A_{PV}^T(\beta) = \max \sum_{i=1}^{N_{MS}(\beta)} W \cdot L \quad (7)$$

where A_{PV}^T in (m²) is the total area of the PV modules, L in (m) is the length of a mounting system, W in (m) is the width of a mounting system, and N_{MS} is the number of mounting systems. The constraints that the objective function has to fulfill are the following:

- (i) Clamps are used to fix the PV modules to the mounting system. Therefore, a transversal installation distance (e_t) between PV modules has been considered;
- (ii) A longitudinal installation distance (e_l) between mounting systems must be considered. This parameter will be an algorithm output. PV system designers use different assumptions to define the minimum distance (e_l^{st}) between row to row of mounting systems (Bey et al., 2021; Yadav and Mukherjee, 2021). Numerous legislations also require a minimum separation (e_l^{st}) between rows of mounting systems to minimize the self-shading of PV modules. For example, the Spanish Government Technical Report states that to minimize the self-shading of PV modules the distance between neighboring rows of mounting systems has to guarantee a minimum of four hours of sunshine around noon on the winter solstice (IDAE, 2011). In this work and as shown in Fig. 2b, the longitudinal incidence angle (θ_{l0}) that minimizes shading effects will be defined, where it can be determined at noon or at any time before the shortest day of the year (21 December for the northern hemisphere) (Brelc and Topič, 2011), and it can be identified using Eq. (8). According to the Spanish Government Technical Report (IDAE, 2011) and as shown in Fig. 2(a-b), e_l^{st} is given by Eq. (9). A longitudinal maintenance distance (e_l^m) between neighboring rows of mounting systems is also necessary for cleaning and maintenance operations (Byrne et al., 2015), where it is found that Byrne et al. have provided a Table showing the relationship between the tilt angle to the longitudinal maintenance distance (e_l^m) (please see Table 9 in Ref. Byrne et al. (2015)). Regarding the longitudinal installation distance e_l between mounting systems, it is determined as the maximum of e_l^{st} and e_l^m (see Eq. (10));
- (iii) It is necessary to consider a minimum distance (e_b) between the rooftop boundary and the PV modules for maintenance operations and foot traffic;
- (iv) It is also necessary to consider a minimum distance (e_b') between the building components and the PV modules for maintenance operations and foot traffic.

$$\theta_{l0} = \arctan[\tan \theta_z \cos \gamma_s] \quad (8)$$

$$e_l^{st} = S \frac{\tan \beta}{\cot \theta_{l0}} = L \frac{\sin \beta}{\cot \theta_{l0}} \quad (9)$$

$$e_l = \max[e_l^{st}, e_l^m] \quad (10)$$

The problem consists in packing rows of mounting systems with a south orientation, without solar tracking system, in the East–West direction inside the available rooftop area (\bar{P}), where these rows of mounting systems have the following characteristics: Southwards orientated, tilt angle β , different configurations, length L , and width W . As shown in Fig. 5 and Eqs. (11) and (12), to facilitate the application of the packing algorithm, the elements used shall be the projection of each mounting system on the horizontal plane (R_{ij}).

$$\Delta x = W + e_t; \quad \Delta y = S + e_l \quad (11)$$

$$R_{ij} : \{ A((j-1)\Delta x, (i-1)\Delta y), B((j-1)\Delta x + W, (i-1)\Delta y), \quad (12)$$

$$C((j-1)\Delta x + W, (i-1)\Delta y + S), D((j-1)\Delta x, (i-1)\Delta y + S) \}$$

With this packing algorithm, it is necessary to check whether a mounting system belongs to the available rooftop area (\bar{P}). For this purpose, the minimum distance of the four vertices of each R_{ij} to the complementary region (\overline{CP}) of \bar{P} is calculated in the Mathematica™ software using Eq. (13) with the restriction $\geq e_b$.

$$\overline{CP} = \text{DiscretizeRegion}[\text{RegionDifference}[\mathbb{R}^2, \bar{P}]] \quad (13)$$

$$\text{Min}[\text{RegionDistance}[\overline{CP}, R[i, j]]] \geq e_b \quad (14)$$

As shown in Eq. (15), the studied algorithm also takes into account the building components ($CE_i, i = 1, 2, \dots$, etc.). For this purpose, the above procedure can be used to calculate the new parcel.

$$\overline{P}^* = \text{RegionDifference}[\overline{P}, CE_1, CE_2, \dots] \quad (15)$$

As shown in Eq. (16), another possible implementation, perhaps more versatile and general, is to calculate the minimum distance between two regions with the assumption that it is $\geq e_b$.

$$\text{MinValue}[\text{EuclideanDistance}[x, y], \{x \in CE_i, y \in \text{Polygon}[R[i, j]]\}] \geq e_b \quad (16)$$

To study the irregular shape rooftop, the algorithm chooses different points for the vertex A of R_{11} inside the area ($\Delta x \times \Delta y$) highlighted in Fig. 5. The algorithm analyses m^2 possible combinations ($l, k = 1, 2, \dots, m$) and provides for each tilt angle β (and each mounting system configuration) the best packing and also calculates the maximum number of mounting systems $n_r(\beta)$ and how many of them are never affected by shadows, $n_{ms}(\beta)$, i.e. the first to receive the sunlight from the South.

3.2. Determination of operating periods of the PV system

Determining the operating periods of the PV system is essential to determine the effective area of the PV modules and to maximize the annual effective energy event on them. Therefore, at sunrise time $T_R(n)$ and sunset $T_S(n)$, the solar irradiance does not reach the effective surface of the PV modules due to self-shading, which results in a loss in the effective area of the PV modules (Self-shading losses). In addition, sometimes it is noticed that the solar irradiance reaches the back surface of the PV modules (sun faces towards the rear face of the PV module), which it results in a direct decrease in the hourly power incident that leads to a decrease in the annual effective energy incident on the PV modules.

3.2.1. Self-shading losses

Solar PV systems consist of a number of solar panels wired into arrays depending on the demand for electrical energy from each of those panels, which, in turn, consist of many solar PV cells that are the basic units involved in capturing energy from the sun and converting it into electricity. Now, if the shade falls on even just one part of the solar panels in the array, the output from the entire system may be compromised, this can be referred to as PV panel shading. With parallel arrayed PV mounting systems, the self-shading of the modules may be caused by the array of modules. In these cases, it is necessary to improve the slope and separation of the module rows so that the solar irradiance can reach the entire effective area of the PV system. Therefore, it is important to determine the period $[T_1(n), T_2(n)]$ of the day in which there is no effect of shading of the photovoltaic rows on each other. This period is called the PV system operating hours, and they are in terms of (θ_{l0}) per day (n), where shading occurs when ($\theta_l > \theta_{l0}$) as shown in Fig. 2b.

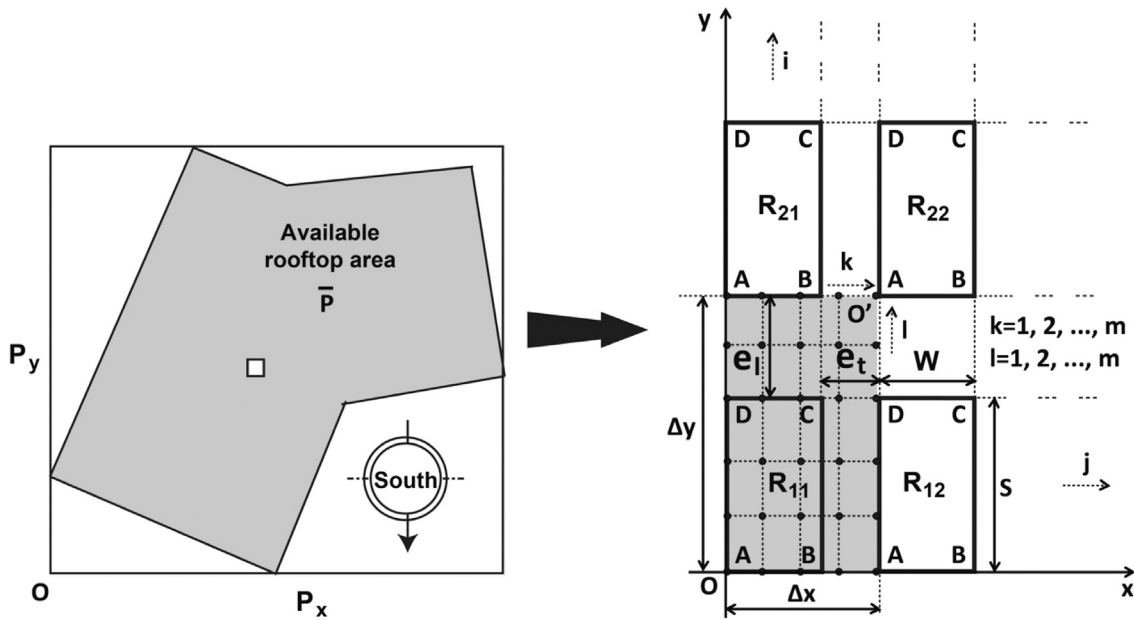


Fig. 5. Packing algorithm.

3.2.2. Sun faces towards the rear face of the PV module

Sun faces towards the rear face of the PV module when $\cos \theta_i$ is negative, where it can be calculated using Eq. (17) (Duffie and Beckman, 2013).

$$\begin{aligned} \cos \theta_i = & \sin \delta \cdot \sin \lambda \cdot \cos \beta - \sin \delta \cdot \cos \lambda \cdot \sin \beta \cdot \cos \gamma \\ & + \cos \delta \cdot \cos \lambda \cdot \cos \beta \cdot \cos \omega \\ & + \cos \delta \cdot \sin \lambda \cdot \sin \beta \cdot \cos \gamma \cdot \cos \omega + \cos \delta \cdot \sin \beta \cdot \sin \gamma \cdot \sin \omega \end{aligned} \quad (17)$$

where δ in ($^\circ$) is the solar declination, λ in ($^\circ$) is the latitude, γ in ($^\circ$) is the azimuth angle, and ω in ($^\circ$) is the hour angle. In the case of South-facing PV modules, Eq. (18) that proposed by Duffie and Beckman can be used to determine the time for which $\cos \theta_i$ is non-negative (Duffie and Beckman, 2013).

$$\cos \theta_i = \cos(\lambda - \beta) \cdot \cos \delta \cdot \cos \omega + \sin(\lambda - \beta) \cdot \sin \delta = 0 \quad (18)$$

Therefore, it is immediate to determine the hour angle (ω) analytically using Eq. (18). From there, it is possible to determine the range of hours of the day $[T_a(n), T_b(n)]$ in which $\cos \theta_i$ is non-negative.

Therefore, the day can be divided into three time periods: $[T_R(n), T_S(n)]$ in which there is sunlight, $[T_1(n), T_2(n)]$ in which there is no self-shading loss, and $[T_a(n), T_b(n)]$ in which the sun faces the front of the PV module.

Fig. 6 shows the different operating periods of the PV system for a certain (β). The intersection point of the three operational periods is $n = 80$ and $n = 267$ (marked in Fig. 6 with an orange line). $\cos \theta_i$ becomes negative when the sun's azimuth (γ_S) falls outside the range $[-90^\circ, 90^\circ]$, where this happens after sunrise and before sunset on certain days of the year, precisely when the solar declination (δ) changes from negative to positive (or vice versa.), on March 21 ($n = 80$) and September 21 ($n = 267$) of the year.

Therefore, there are three calculation zones based on Fig. 6 and they are as follows: zone A ($1 \leq n \leq 80$), zone B ($81 \leq n \leq 266$), and zone C ($267 \leq n \leq 365$). In zones A and C, the energy is determined between $[T_R(n), T_S(n)]$ and it is determined between $[T_a(n), T_b(n)]$ in zone B.

In terms of effective area, the green zone in Fig. 6 represents the time without shadow losses, while the gray area shows the time when there are losses in the effective area of the photovoltaic modules.

3.3. Calculation of the effective area of PV modules

As shown in Fig. 2b, the effective area of the PV module is the front area of the PV module illuminated by the sun, where Eq. (19) allows calculating the shaded value B in (m) of the PV module.

$$B(n, \beta, T) = \frac{\sin(\theta_l - \theta_{l0})}{\cos(\beta - \theta_l)} L \sin \beta \sec \theta_{l0} \quad (19)$$

According to Fig. 6 and in the green area, Eq. (20) allows calculating the effective area A_{PV}^E of PV modules.

$$A_{PV}^E(n, \beta, T) = A_{PV}^T(\beta) \quad (20)$$

While Eq. (21) allows calculating the effective area in the gray area of Fig. 6.

$$A_{PV}^E(n, \beta, T) = A_{PV}^T(\beta) - W \cdot B(n, \beta, T) \cdot (N_{MS}(\beta) - N_{MSns}(\beta)) \quad (21)$$

where N_{MS} is the number of mounting systems and N_{MSns} is the number of mounting systems not shaded.

3.4. Maximization of effective annual energy incident on PV modules

Eq. (22) allow calculate the effective annual energy incident on PV modules installed on the rooftop.

$$E_{PV}(n, \beta) = \int_{h_R(n)}^{h_S(n)} \mathbb{I}_t(n, \beta, T) \cdot A_{PV}^E(n, \beta, T) dT \quad (22)$$

where $h_R(n)$ and $h_S(n)$ can take the following values $T_R(n), T_S(n), T_1(n), T_2(n), T_a(n)$ and $T_b(n)$ depending on the operation zone.

Therefore, $E_{PV}(n, \beta)$ can be calculated according to the zones shown in Fig. 6 as follows:

- (i) For zones A and C, Eq. (23) is used.

$$E_{PV}(n, \beta) = \int_{T_R(n)}^{T_1(n)} \mathbb{I}_t \cdot A_{PV}^E dT + A_{PV}^T \int_{T_1(n)}^{T_2(n)} \mathbb{I}_t dT + \int_{T_2(n)}^{T_S(n)} \mathbb{I}_t \cdot A_{PV}^E dT \quad (23)$$

- (ii) For zone B, Eq. (24) is used.

$$E_{PV}(n, \beta) = A_{PV}^T \int_{T_a(n)}^{T_b(n)} \mathbb{I}_t dT \quad (24)$$

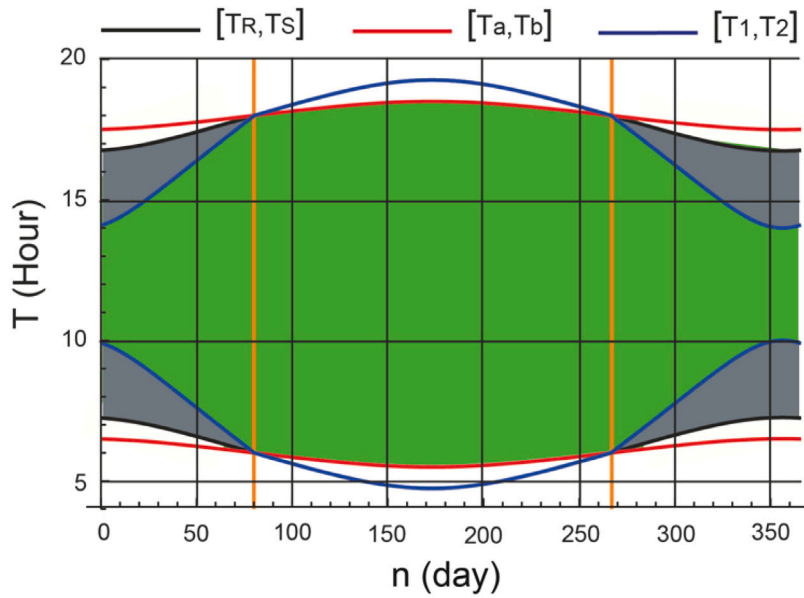


Fig. 6. Operating hours of the PV system.

Finally, Eq. (25) gives the total annual energy received by the PV modules for each tilt angle β .

$$E_a(\beta) = \sum_{n=1}^{365} E_{PV}(n, \beta) \quad (25)$$

So, from the curve $E_a(\beta)$ in (Wh/year), the optimum tilt angle (β^*) is immediately deduced for each mounting system configuration.

4. Efficacy assessment

We evaluate the efficiency of each deployment of rows of PV modules on the rooftop in relation to the optimal PV module layout, in three aspects: the PV field area gain, the energy gain, and the levelized cost of the electrical energy (LCOE).

4.1. PV field area gain

The PV field area gain (PVAG) can be calculated as the difference between the PV field area obtained by the optimal PV module layout (β^*) and the specific deployments of rows of PV modules on the rooftop (β), as a % of area:

$$PVAG = \frac{A_{PV}^T(\beta^*) - A_{PV}^T(\beta)}{A_{PV}^T(\beta)} \cdot 100 \quad (26)$$

4.2. Energy gain

In this study, different deployments of rows of PV modules on the rooftop will be compared in terms of the energy gain (Bahrami et al., 2017). The energy gain (EG) can be calculated as the difference between the energy absorbed by the optimal PV module layout (β^*) and the specific deployments of rows of PV modules on the rooftop (β), as a % of energy:

$$EG = \frac{E_a(\beta^*) - E_a(\beta)}{E_a(\beta)} \cdot 100 \quad (27)$$

4.3. LCOE

The levelized cost of electricity produced (LCOE) is used to compare the unit cost of electricity generated by different deployment of photovoltaic module rows on rooftop over their lifetime. Allouhi et al.

(2019) define the LCOE as the ratio between the life-cycle cost of the PV system and the energy produced over its lifetime, and provide Eq. (28) for its calculation.

$$LCOE = \frac{\sum_{i=0}^I [C_i / (1+r)^i]}{\sum_{i=0}^I [Q_i / (1+r)^i]} \quad (28)$$

where C_i in (€) is the net cost of the project for i , Q_i in (kWh) is the total electrical energy output for i , I in (years) is the lifetime of the project, r is the discount rate for i , and i is the year. The net cost of the project of a PV system is the sum of the initial investment cost, the operating and maintenance costs and the interest expenditure if it is debt financed.

An adaptation of the equation provided by Khalil Zidane et al. (2019) for the calculation of the initial investment cost can be used for a rooftop PV system. The equation used in this study is as follows:

$$C_i = N_{PV} \cdot C_{PV} + N_{inv} \cdot C_{inv} + N_{MS} \cdot C_{MS} + C_{cb} + C_{pd} \quad (29)$$

where N_{PV} is the total number of PV modules, C_{PV} in (€/unit) is the unit cost of a PV module, N_{inv} is the total number of inverters, C_{inv} in (€/unit) is the unit cost of the inverter, N_{MS} is the total number of mounting systems, C_{MS} in (€/unit) is the unit cost of the mounting structure, C_{cb} in (€) is the cost of the cable, and C_{pd} in (€) is the cost of the protection devices.

Although there is no standardized annual operating and maintenance cost (Talavera et al., 2019), the National Renewable Energy Laboratory report (NREL, 2018) estimate these costs at approximately 0.5% and 1% of the initial investment for large and small systems, respectively.

The electricity generated each i th year can be calculated by (Allouhi et al., 2019):

$$Q_i = E_{ai} \cdot \eta \cdot (1-d)^i \quad (30)$$

where Q_i in (kWh) is the total electrical energy output at the i th year, E_{ai} in (kWh) is the availability of solar resource at the i th year, η is the performance factor, d is the annual degradation rate, and i is the year.

Similar work uses LCOE efficiency to compare different mounting system configurations (Barbón et al., 2021). LCOE efficiency is introduced as the ratio between the LCOE $_{\beta^*}$ with optimal PV module

Table 1
10 commercial PV modules.

n°	Manufacturer	PV model	Technology	W_{PV}	L_{PV}
1	Era Solar (ES)	BSP275P	Polycrystalline (P)	991	1640
2	Era Solar (ES)	ESPMC	Polycrystalline (P)	992	1650
3	Solar Power (SP)	REC TWIN PEAK	Polycrystalline (P)	997	1675
4	Era Solar (ES)	ESPMC	Monocrystalline (M)	990	1650
5	Era Solar (ES)	ESPMC	Monocrystalline (M)	1002	1665
6	Talesun (TS)	TP672P	Monocrystalline (M)	992	1960
7	Era Solar (ES)	ESPMC	Polycrystalline (P)	992	1956
8	Era Solar (ES)	ESPMC	Monocrystalline (M)	1002	1979
9	Jinko Solar (JS)	HC 72 M	Monocrystalline (M)	1002	2008
10	JA Solar (JA)	MBB HALF-CELL	Monocrystalline (M)	1052	2120

layout (β^*) and the $LCOE_\beta$ with PV module layout with any tilt angle (β):

$$\eta_{LCOE} = \frac{LCOE_{\beta^*}}{LCOE_\beta} \quad (31)$$

Notice that an η_{LCOE} value less than 1 implies that the PV module layout with any tilt angle (β) is less efficient than the optimal PV module layout (β^*).

5. Methodology application and results analysis

The objective of this section is to verify the feasibility of the proposed methodology. For such methodology application, an irregular rooftop shape, a given study location, and 10 commercial PV modules were used as the starting point. This study determined the parameters necessary for the optimal design of a flat rooftop PV system to maximize the amount of energy captured by all the PV modules, i.e., number and arrangement of mounting systems, mounting system configuration, dimensions of commercial PV modules, the tilt angle of mounting system, and distance between rows of mounting systems. The optimization algorithm has been implemented with specific Mathematica™ code.

5.1. Base case

The base case is determined by the flat rooftop shown in Fig. 1. The available rooftop area (\bar{P}) is 1129.97(m²). The dimensions of the rectangle (\bar{R}) where \bar{P} is inscribed are 45.65 × 42.8(m). The building components have the following dimensions $L_{BC} \times W_{BC} = 1.20 \times 1.45$ (m), while its height is 2.5(m), e.g. a lift. The shadow caused by the building components will be disregarded in this study, as it has almost no influence on the total size of the terrace. Furthermore, the shading effect is negligible when considering the distance between building components and PV modules. The rooftop is located in Almería (Spain), which has a latitude of 36°50'07"N, a longitude of 02°24'08"W, and an altitude of 22(m).

The algorithm calculates the commercial PV module that best suits the needs of each rooftop. Based on the work of Belsky et al. who analyzed 1300 PV modules (Belsky et al., 2022), 10 types of PV modules from five manufacturers were selected in this study. Table 1 shows general information such as the PV manufacturer, the PV model, the technology used, as well as the length W_{PV} in (mm) and width L_{PV} in (mm) of the selected PV module.

Although the mounting system configuration is an output of the algorithm, it can vary between four possible configurations: 1V, 1H, 2V, and 2H. While 3H and 3V configurations are discarded due to their excessive height. There is a possibility of 40 different combinations of $W \times L$.

5.2. Methodology application

For the implementation of this methodology, the four proposed steps have been applied to the base case: (i) Maximization the total area of the PV modules; (ii) Determination of operating periods of a PV system; (iii) Calculation of the effective area of PV modules; and (iv) Maximization of effective annual energy incident on PV modules. The final result is the optimal solution, i.e. the PV module model used, the optimal arrangement of the PV modules, the number of mounting systems and their configuration, and the tilt angle of the PV modules.

5.2.1. Step 1: Maximization of total PV modules area $A_{PV}^T(\beta)$

Initially, the following parameter values are selected:

- (i) The transversal installation distance (e_t) is 0.025 (m);
- (ii) The longitudinal maintenance distance (e_l^m) is 1 (m);
- (iii) The distance between the rooftop boundary and the PV modules (e_b) is 1 (m);
- (iv) The distance between the building components and the PV modules (e_b') is 1 (m).

Then the longitudinal installation distance (e_l) is chosen according to Eq. (10), where (e_l^s) must be calculated for each of the combinations ($W \times L$) and tilt angle (β).

Regarding the solar longitudinal incidence angle (θ_{10}), it is determined using the classical solar geometry formula (Duffie and Beckman, 2013) and the imposition of the IDAE standard (IDAE, 2011). For the location of Almería in Spain, θ_{10} is equal to 63.37 (°).

Fig. 7 shows the optimal total modules area $A_{PV}^T(\beta)$ as a function of tilt angle (β), where it has been constructed with the 40 different combinations of mounting systems and PV modules. The tilt angle range has been chosen based on experience from other work. In this case, the tilt angle range is $\beta \in [5^\circ, 34^\circ]$. These values are merely an example, without loss of generality. In addition to the optimal total modules area, the algorithm provides all the characteristics of the optimal solution, i.e., the number of rows of mounting systems, the number of PV modules per row, the specific placement of each mounting system, the distance between rows and of course the optimal mounting system configuration for each tilt angle. This detailed information is shown in Table 2, where the number in brackets with the mounting system configuration is the number of the commercial PV module listed in Table 1.

Table 2 shows that the number (n°) of the commercial PV module varies randomly over the range of tilt angle values. However, the type of mounting system configuration varies throughout the range of tilt angle values in a consistent and logical pattern. From Table 2 it is noted that:

- (i) For low tilt angle values (β up to 12 (°)), the 2V mounting system configuration proves to be the most effective in maximizing the total PV modules area. Although this configuration has 2 rows of PV modules per mounting system, the low tilt angle (β) means that the shadow produced is less than the required maintenance distance between rows (e_l^m), thus complying with the restriction imposed;
- (ii) For the same reason mentioned in the previous point, the 1V configuration is the best solution for tilt angle values in the range between ($13^\circ \leq \beta \leq 33^\circ$). For these tilt angles, the 2V configuration has a high height and requires an excessive distance (e_l^s) to comply with the standard;
- (iii) Finally, for the tilt angle value ($\beta = 34$ (°)), the 2H mounting system configuration is the best.

The results shown in Table 2 illustrate the importance of this study, as it is not possible to predict the optimal configuration easily.

Another interesting aspect is determining the parameter (m) (see Fig. 5). The choice of this parameter is directly related to the execution

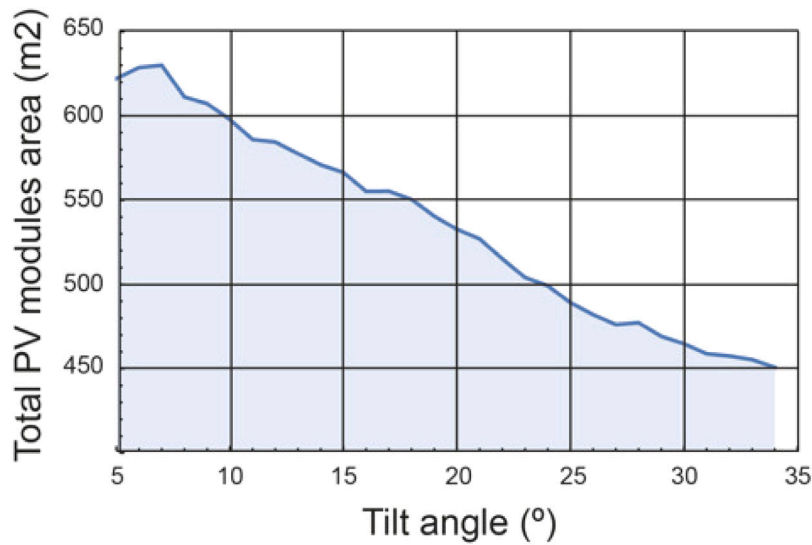


Fig. 7. The total PV modules area $A_{PV}^T(\beta)$.

Table 2
Optimal solution A_{PV}^T (m²) and optimal mounting system configuration.

β (°)	$A_{PV}^T(\beta)$	MS config.	β (°)	$A_{PV}^T(\beta)$	MS config.	β (°)	$A_{PV}^T(\beta)$	MS config.
5	622.182	2V (n° 6)	15	566.481	1V (n° 10)	25	489.197	1V (n° 1)
6	628.674	2V (n° 7)	16	555.228	1V (n° 8)	26	482.147	1V (n° 5)
7	629.960	2V (n° 6)	17	555.330	1V (n° 10)	27	476.195	1V (n° 1)
8	611.211	2V (n° 3)	18	550.490	1V (n° 4)	28	477.271	1V (n° 10)
9	607.272	2V (n° 5)	19	540.539	1V (n° 5)	29	469.263	1V (n° 3)
10	597.851	2V (n° 3)	20	532.722	1V (n° 3)	30	464.851	1V (n° 2)
11	585.974	2V (n° 2)	21	527.050	1V (n° 2)	31	458.860	1V (n° 6)
12	584.491	2V (n° 3)	22	515.201	1V (n° 1)	32	457.573	1V (n° 3)
13	577.632	1V (n° 10)	23	504.134	1V (n° 2)	33	455.454	1V (n° 5)
14	570.941	1V (n° 10)	24	499.224	1V (n° 2)	34	450.846	2H (n° 4)

time of the proposed algorithm. After many times of simulations, it has been concluded that the optimum value of (m) is 3. In other words, 9 combinations are made, starting from different origin points for vertex A of the rectangle pattern R_{11} . This value is a compromise solution between the computational cost of a higher (m) and achieving sufficient accuracy for very irregular rooftop shapes. In this respect, it should be noted that this methodology step consumes a lot of CPU time. For this example, the algorithm running time is around 90 (min) on a personal computer (Intel Core, i5 – 1035G1CPU, 1.00 GHz).

5.2.2. Step 2: determination of operating periods of the PV system

In this step of the methodology, the influence of the operating periods of the PV system will be analyzed, as the operational periods of the PV system depend on (β).

The operating range of the PV system without self-shading $[T_1(n), T_2(n)]$ depends on the value of θ_{10} , whereas, in this study, it was determined according to criterion standard IDAE (2011). Therefore, for the location of Almería (Spain), $\theta_{10} = 63.37$ (°). The values of the solar time $T_1(n)$ and $T_2(n)$ for each day of the year can be determined using Eq. (8). For example, for $\beta = 20$ (°) and $n = 1$, the values of $[T_1(n), T_2(n)]$ are [9.89, 14.11] and for $\beta = 20$ (°) and $n = 70$, their values are [6.20, 17.80]. For $n = 1$, $[T_R(1), T_S(1)] = [7.24, 16.76]$, so the effective area is determined between the time ranges $[T_R(1), T_S(1)]$ and $[T_a(1), T_b(1)]$, and this deduction is correct and valid for n between $1 \leq n \leq 80$ and $267 \leq n \leq 365$ (i.e., in the operating zone A and C). But when the declination (δ) is positive (i.e. when $80 < n < 267$ (i.e., in the operating zone B)), no self-shading at any time of the day, i.e. $[T_R(n), T_S(n)] = [T_1(n), T_2(n)]$.

Eq. (18) can be used to determine the interval $[T_a(n), T_b(n)]$ in which the sun faces the front face of the PV module ($\theta_i = [0^\circ, 90^\circ]$). For

example, $[T_a(1), T_b(1)] = [6.49228, 17.5077]$ for $\beta = 20$ (°) and $n = 1$, and $[T_a(140), T_b(140)] = [5.58376, 18.4162]$ for $\beta = 20$ (°) and $n = 140$. For $n = 1$, $[T_R(1), T_S(1)] = [7.24, 16.76]$, so the energy is determined in the range time $[T_R(1), T_S(1)]$ since this value is less than $[T_a(1), T_b(1)]$, and this deduction is correct and valid for (n) between $1 \leq n \leq 80$ and $267 \leq n \leq 365$ (i.e., in the operating zone A and C). Since for $\beta = 20$ (°) and $n = 140$, it is satisfied that $[T_R(140), T_S(140)] = [4.95778, 19.0422]$, so the energy is determined between $[T_a(140), T_b(140)]$ since this value is less than $[T_R(140), T_S(140)]$, and this deduction is correct and valid for between $80 < n < 267$ (i.e., in the operating zone B).

Fig. 8(a–b) show the operating periods for $\beta = 20$ (°) and $\beta = 10$ (°), respectively, where the intersection point of the three operating periods is at $n = 80$ and $n = 267$ (In Fig. 8(a–b), the coordinates of the intersection between the three operating periods are highlighted in orange). By comparing the two Figures 8a and 8b, the following is observed:

- (i) Obviously, the operating period $[T_R(n), T_S(n)]$ is the same for both cases studied ($\beta = 20$ (°) and $\beta = 10$ (°));
- (ii) The tilt angle variation (β) has a little influence on the operating period $[T_1(n), T_2(n)]$;
- (iii) The tilt angle variation (β) has an appreciable influence on the operating period $[T_a(n), T_b(n)]$. The smaller the tilt angle of the PV module, the lower the incidence of the sun’s rays on the rear of the PV module.

5.2.3. Step 3: Calculation of the effective area of PV modules

As mentioned earlier, knowing the values of shading $B(n, \beta, T)$ will allow to know the effective area (Once $B(n, \beta, T)$ is determined, the effective area can be determined by Eq. (21)), and from there knowing

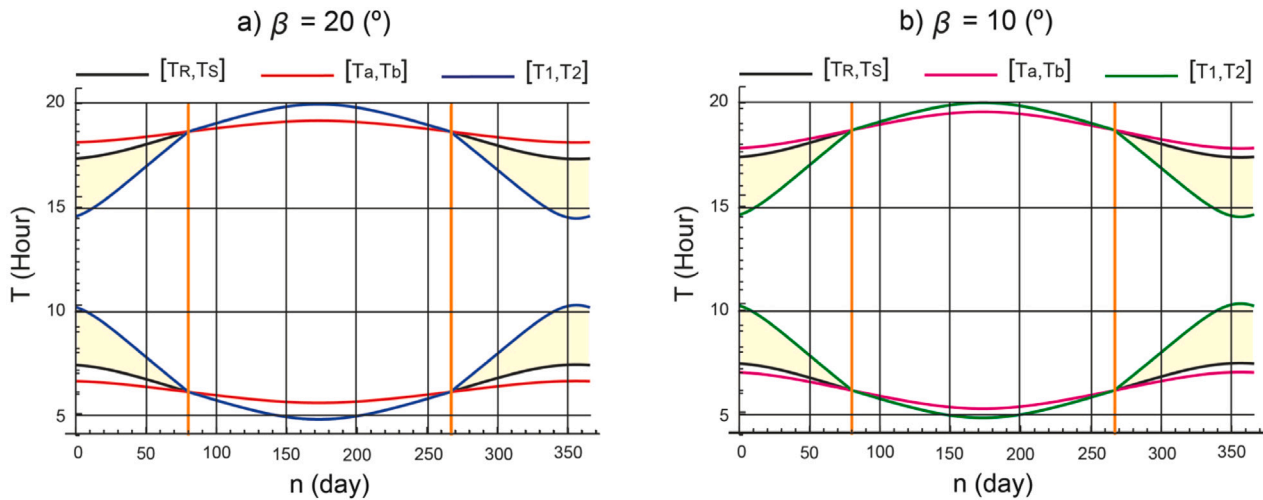


Fig. 8. Operating hours of the PV system for $\beta = 20^\circ$ and $\beta = 10^\circ$.

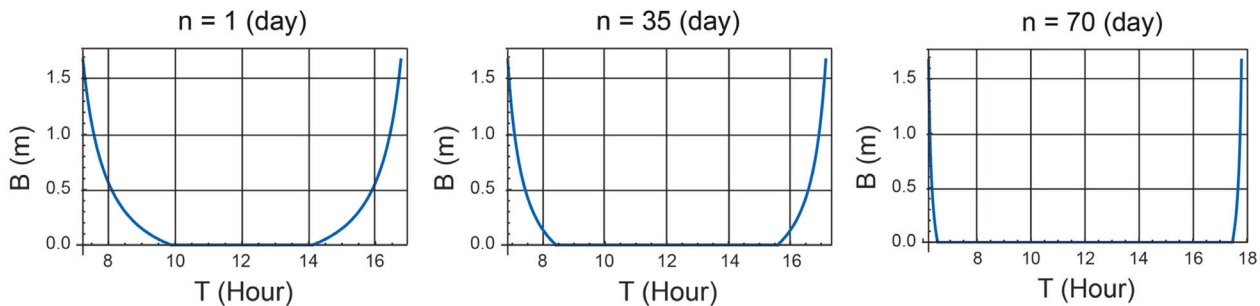


Fig. 9. Shading Variation $B(n, 20^\circ, T)$.

the amount of solar irradiance received annually by the PV modules as shown in Eq. (22). Since the shading $B(n, \beta, T)$ depends on three variables, its graphical representation must be limited to a few concrete examples. Without loss of generality, the tilt angle ($\beta = 20^\circ$) has been chosen to analyze the evolution of (B) for different days of the year n against solar time (T). According to Table 2, the optimum solution for a tilt angle of 20° is $1V$ ($n^{\circ}3$) with mounting system dimensions of $W \times L = 0.997 \times 1.675$ (m).

Fig. 9 shows the shading on days 1, 35 and 70. For $n = 1$, it follows that $[T_R(1), T_S(1)] = [7.24, 16.76]$ and $[T_1(1), T_2(1)] = [9.89, 14.11]$. Therefore, the shading occurs over a significant time interval (gray zone in Fig. 6) in a smooth and progressive manner, until the maximum value is reached $B = L = 1.675$ (m) at sunrise and sunset.

As the days approach the Spring Equinox ($n = 80$), the shading phenomenon occurs over shorter periods. For example, for $n = 35$, it is satisfied that $[T_R(35), T_S(35)] = [6.85, 17.15]$ and $[T_1(35), T_2(35)] = [8.41, 15.58]$, while it is already almost instantaneous for $n = 70$ because $[T_R(70), T_S(70)] = [6.20, 17.80]$ and $[T_1(70), T_2(70)] = [6.53, 17.46]$. As already mentioned, the days ($n \in [81, 266]$) that marked by vertical orange lines in Fig. 6 are never shaded.

5.2.4. Step 4: Maximization of effective annual energy incident on PV modules

In this last step, the optimum tilt angle will be decided by taking the effective annual energy received by the PV modules as an objective function. To achieve that, it is necessary to calculate the total solar irradiance on a tilted plane using Eq. (6), where the beam and diffuse solar irradiance on the horizontal plane have to be determined taking into account the climatic conditions of the site chosen to conduct the study.

Therefore, the optimization algorithm was implemented with a specific Mathematica™ code, where the adjusted beam radiation (I_{bh}) and diffuse radiation (I_{dh}) received by the horizontal plane, was calculated using the method presented by Barbón et al. (2020). Regarding this method for calculating the amount of solar irradiance, it takes into account the effect of particular weather conditions, where PVGIS data has been used to obtain a package with average monthly and diffuse solar irradiance (PVGIS, 2022). Consequently, Fig. 10 shows the three-dimensional plot of the $E_{PV}(n, \beta)$, as it was obtained using Eqs. (23) and (24).

To get the optimal tilt angle (β) and as shown in Fig. 11, Eq. (25) has been used to calculate the total annual energy $E_a(\beta)$ for each tilt angle (β).

From Fig. 11, it is noted that the tilt angle ($\beta = 7^\circ$) gives the greatest amount of annual energy $E_a = 1240.12$ (MWh) received by the studied PV modules, so the title angle $\beta^* = 7^\circ$ is the optimal tilt angle for the studied PV modules.

The most important conclusion of the study is that the adoption of the tilt angle of the PV modules less than the optimal tilt angle ($\beta < 7^\circ$), will allow receiving significant amounts of the total energy received from the PV system. Although the tilt angle of each PV module alone is not optimum, many more PV modules can be installed (within all constraints), and the total energy, taking into account the self-shading effect, is much higher. For each specific example, the algorithm allows finding the tilt angle for the optimal arrangement of the PV modules.

5.2.5. Optimal solution

Finally, all that remains is to return to step 1 of the methodology and present the final solution.

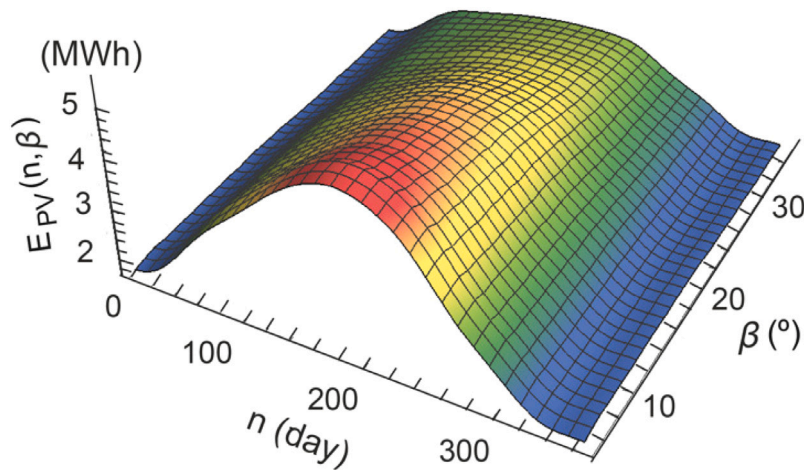


Fig. 10. Effective energy $E_{PV}(n, \beta)$.

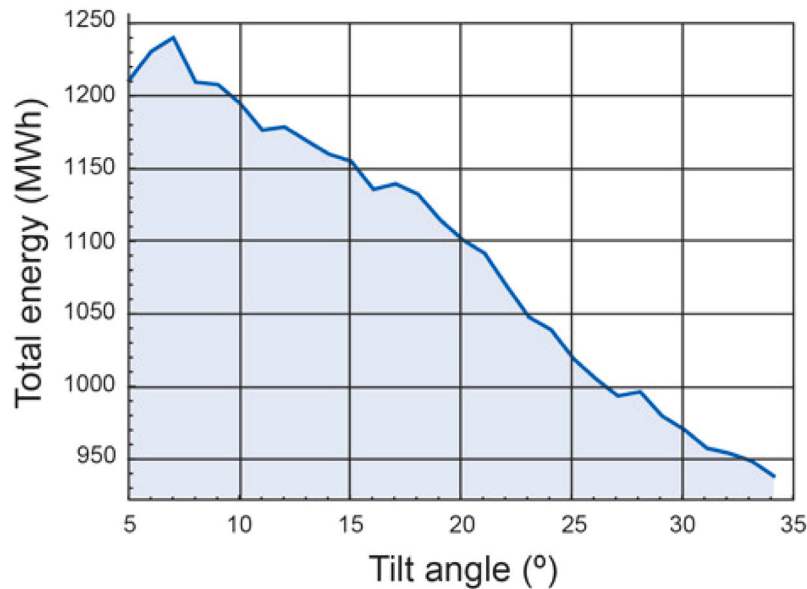


Fig. 11. Maximization of effective annual energy $E_a(\beta)$.

Fig. 12 shows the optimal arrangement of the PV modules, whereas, PV modules of model $n^{\circ}6$ (TP672P) were used (i.e., $W_{PV} \times L_{PV} = 0.992 \times 1.96$ (m), this means, $W \times L = 0.992 \times 3.92$ (m)). The optimal PV system consists of 162 mounting systems using 2V configuration (i.e., $A_{PV}^T = 629.96$ (m²)), where the tilt angle of the PV modules is ($\beta^* = 7$ (°)). Therefore, there are 39 mounting systems without self-shading because they are in the first row facing South. The longitudinal installation distance between mounting systems is $e_l = e_l^m = 1$ (m), simultaneously verifying the standard IDAE (IDAE, 2011). Also, it can be seen how the optimal solution respects the distance between the rooftop boundary and the PV modules, and the distance between the building components and the PV modules ($e_b = e_b' = 1$ (m)).

5.3. Efficacy assessment

To highlight the importance of this study and how it differs from other studies, many comparisons have been made with previous studies that dealt with the effect of the optimal tilt angle for PV modules on maximizing the solar irradiance received by them.

Assuming the PV modules are South oriented, numerous studies provide estimates of optimum tilt angles in different sites around the world, Barbón et al. (2022) and Chinchilla et al. (2021). These studies

use models that can be classified into two categories: (i) models that use only the latitude angle of the site, and (ii) models based on maximizing the total solar irradiance incident on the tilted surface. Among all these models, three have been selected in this study: (i) IDAE Technical Report (IDAE, 2002), (ii) Lorenzo's Equation (Lorenzo, 2011), and (iii) Jacobson's Equation (Jacobson and Jadhav, 2018). Model (i) has been selected because it is the one recommended by the Spanish government, where the study has been carried out. Model (ii) is commonly used in Spain (Marzo et al., 2018; Fernández-Infantes et al., 2006). And model (iii) is very commonly used in other parts of the world (Nicolás-Martín et al., 2020; Al Garni et al., 2019; Ascencio-Vásquez et al., 2019; Tröndle et al., 2019).

A Technical Report (IDAE, 2002) by IDAE requires that the annual optimum tilt angle be determined by Eq. (32):

$$\beta_{opt} = \lambda - 10 \tag{32}$$

where λ is the latitude (°).

For locations with $\lambda < 45^\circ$, Lorenzo (2011) proposes the following equation for calculating the annual optimum tilt angle:

$$\beta_{opt} = 3.7 + 0.69 \cdot |\lambda| \tag{33}$$

Table 3
Relationship between recommended annual optimum tilt angle, A_{PV}^T , and E_a .

Author	Recomm. β ($^\circ$)	$A_{PV}^T(\beta)$ (m^2)	$E_a(\beta)$ (MWh)
IDAE Technical report (IDAE, 2002)	26.8	476.195	993.44
Lorenzo (2011)	29.0	469.263	979.429
Jacobson and Jadhav (2018)	30.0	464.851	970.103

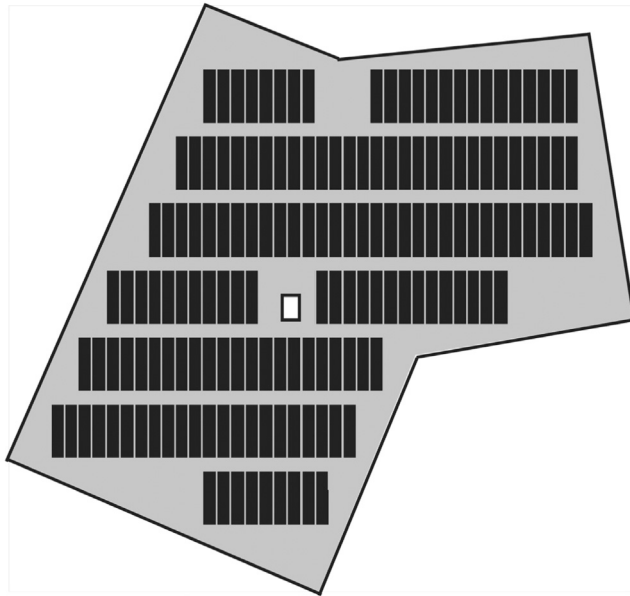


Fig. 12. Optimal distribution of PV modules with $\beta^* = 7$ ($^\circ$).

where λ is the latitude ($^\circ$). This model has been used in Marzo et al. (2018) and Fernández-Infantes et al. (2006).

The Jacobson’s equation (Jacobson and Jadhav, 2018) has also been used extensively (Nicolás-Martín et al., 2020; Al Garni et al., 2019; Ascencio-Vásquez et al., 2019; Tröndle et al., 2019). This model proposes the following equation for calculating the annual optimum tilt angle:

$$\beta_{opt} = 1.3793 + \lambda(1.2011 + \lambda(-0.014404 + 0.000080509\lambda)) \quad (34)$$

where λ is the latitude ($^\circ$).

Table 3 shows the relationship between the photovoltaic modules layout with tilt angle recommended by IDAE Technical Report, Lorenzo’s equation, and Jacobson’s equation and the parameters A_{PV}^T and E_a .

Fig. 13 shows the PV field area gain and energy gain using Eqs. (26) and (27), respectively, for IDAE Technical Report, Lorenzo’s equation and Jacobson’s equation. From Fig. 13 it is clear that the recommended tilt angles (IDAE Technical Report, Lorenzo’s equation and Jacobson’s equation) do not give good results in terms of PV field area gain and energy gain.

In relation to the PV field area gain and the energy gain, Fig. 13 suggests the following conclusions:

- (i) The optimal PV module layout ($\beta^* = 7$ ($^\circ$)) obtains the best results. Although this configuration has the greatest L ($L = 2L_{PV}$) it produces a lower shading because it uses a low tilt angle. Therefore, this configuration packs the most PV modules for the same surface.
- (ii) The Jacobson’s equation gets the worst result. This is due to the fact that it uses a high tilt angle which is close to the site latitude and as a result of this, the produced shadows are very large and the rows of PV modules require more space in between them. Therefore, the use of tilt angles whose values are close to the

latitude value of the site is damaging to the performance of the PV system.

- (iii) The maximum PV field area gain is 35.52% with respect to the Jacobson’s equation and the minimum is 32.29% with respect to the IDAE Technical Report.
- (iv) The maximum energy gain is 27.83% with respect to the Jacobson’s equation and the minimum is 24.84% with respect to the IDAE Technical Report.

Fig. 14 shows the arrangement of the PV modules for optimum tilt angle recommended by IDAE Technical Report, Lorenzo’s equation, and Jacobson’s equation. The parameters obtained are summarized in Table 4.

For the LCOE study, the terms N_{inv} , C_{inv} , C_{cb} , and C_{pd} can be considered to have the same value for all PV module arrangements studied. The price of C_{PV} and C_{MS} have been obtained from Autosolar (2021) (All the cost are referred to date 26/04/2022.). The annual operating and maintenance cost is 0.5% of the initial investment cost (NREL, 2018).

The LCOE efficiency for optimum tilt angle recommended by IDAE Technical Report, Lorenzo’s equation, and Jacobson’s equation is determined using Eq. (31). The η_{LCOE} values are 0.97, 0.98, and 0.97, respectively. Notice that the LCOE of the optimal PV module layout (β^*) is lower than that of the other arrangements studied.

The sensitivity of the model is measured as the influence of the initial investment cost on LCOE efficiency. As the price reduction of photovoltaic modules is the current trend (IRENA, 2017), we consider a price variation of 60% to 100% of the current price. As the price increase of mounting systems is the current trend, we consider a variation of this price between 100% to 140% of the current price. Fig. 15 illustrate our sensitivity analysis. The following conclusions can be inferred:

- (i) The price of the PV modules does not influence the choice of the optimal PV module layout (β^*) as the best option.
- (ii) Only the maximum price (140%) of the mounting systems makes the optimal arrangement of the mounting systems (β^*) more expensive.
- (iii) When the price of PV modules is minimum and the price of mounting systems is minimum, the optimal arrangement of PV modules (β^*) obtains the lowest cost.
- (iv) When the price of the PV modules is maximum and the price of the mounting systems is maximum the optimal arrangement of the PV modules (β^*) obtains the highest cost.

6. Conclusions

This paper presents a general algorithm for the optimization of the deployment of photovoltaic systems installed on irregular flat rooftop shapes, aiming at maximum energy generation.

The main novelty of this algorithm is that it takes into account the limitations posed by other studies, such as:

- (i) Irregular rooftop shape;
- (ii) Self-shading of photovoltaic modules;
- (iii) Inclusion of building components;
- (iv) Commercial photovoltaic modules with different sizes;
- (v) Mounting systems with different configurations.

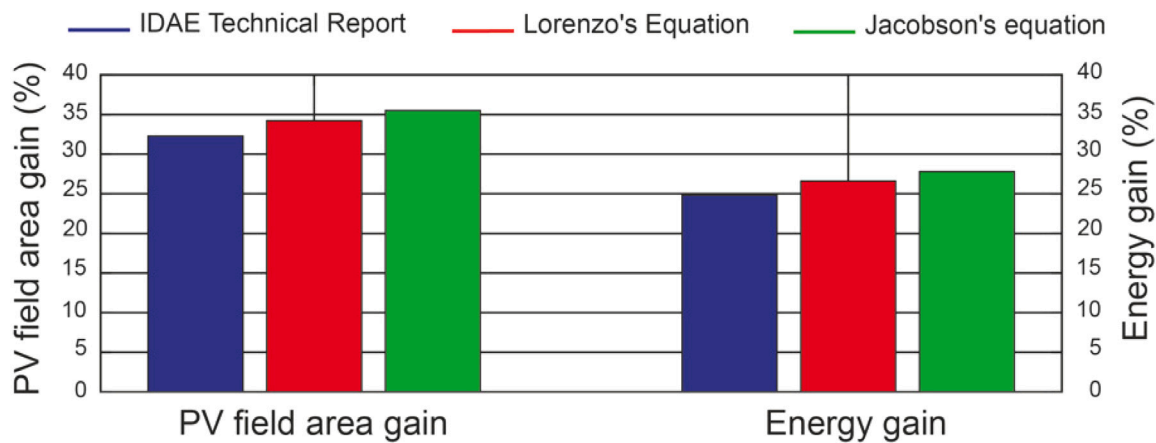


Fig. 13. Ratio of PV field area gain and energy gain with respect to the optimal arrangement of the PV modules for $\beta = 7^\circ$.

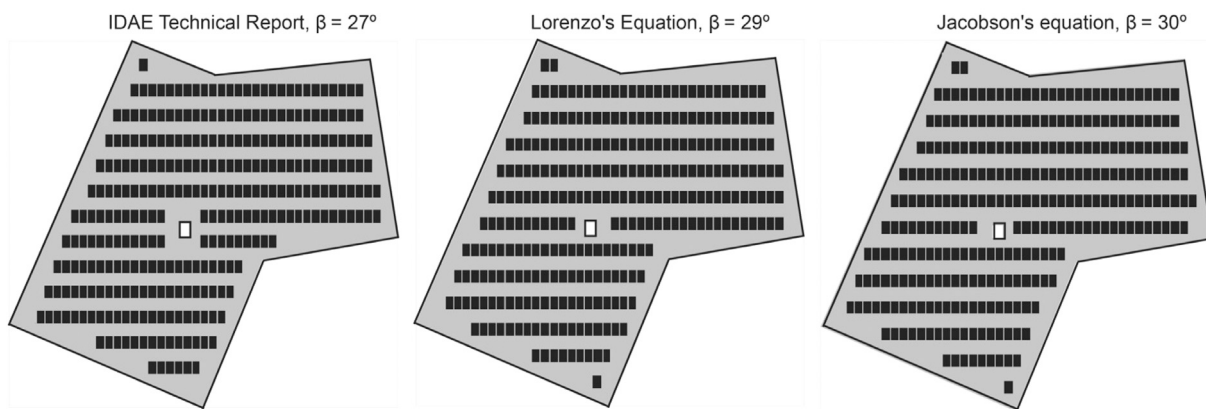


Fig. 14. Arrangement of the PVmodules for optimum tilt angle recommended by IDAE Technical Report, Lorenzo's equation, and Jacobson's equation.

Table 4
Parameters obtained in the study.

Parameters	IDAE (IDAE, 2002)	Lorenzo (Lorenzo, 2011)	Jacobson (Jacobson and Jadhav, 2018)
Recommended β ($^\circ$)	26.8	29.0	30.0
Mounting system config.	1V	1V	1V
PV module model	n°1	n°3	n°2
Number of PV modules	293	281	284
$W_{PV} \times L_{PV}$ (m)	0.992×1.64	0.997×1.675	0.992×1.650
e_l	1.485	1.619	1.645

Decision-makers (i.e., engineers, architects, site managers, owners, etc.) often encounter these issues during the design of the photovoltaics systems in buildings' rooftops. The optimization process is performed by considering the weather conditions of the particular site. The design optimization algorithm is formulated as a constrained packing problem. The optimization algorithm has been implemented with specific Mathematica™ code. To facilitate its replication, the commands used in the development of the code have been introduced. The algorithm used here highlights the important impact of the mounting system configuration and the size of the photovoltaic modules on the row layout. The application of the optimization algorithm results in:

- (i) The optimal number of mounting systems and their configuration;
- (ii) The tilt angle and dimensions of each mounting system;
- (iii) The model of the photovoltaic module;
- (iv) The maximum total photovoltaic modules area;
- (v) The maximum annual incident energy on the photovoltaic modules.

From a qualitative point of view, the study shows the following conclusions:

- (i) The type of mounting system configuration used and its tilt angle have a strong influence on the total photovoltaic modules area. And therefore, on the amount of solar energy captured by the photovoltaic field.
- (ii) The choice of the distance between the mounting systems in the North–South direction is affected by the longitudinal spacing for maintenance, giving more relevance to the type of mounting system configuration used.
- (iii) The total area of the photovoltaic modules shall be maximized when the tilt angle of the mounting systems involves similar values between the longitudinal distance in the North–South direction and the longitudinal spacing for maintenance.
- (vi) Not in all cases, the tilt angle that maximizes the total area of the photovoltaic field is the same as the angle that maximizes the amount of energy captured. Although in most cases they coincide. This difference is due to the cosine of the incidence angle or the Liu and Jordan model for the diffuse and the ground reflected solar irradiance.

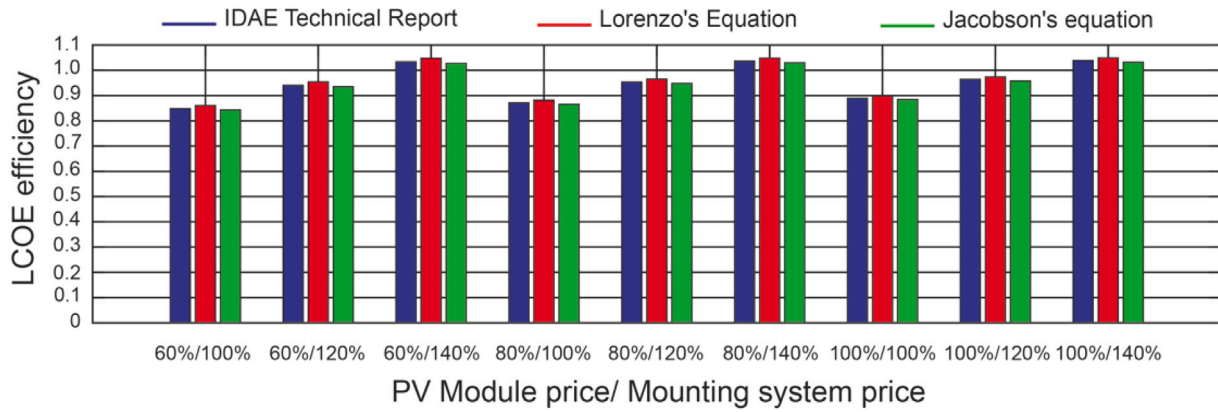


Fig. 15. Sensitivity analysis of LCOE efficiency.

We compare the optimal photovoltaic modules layout with the arrangement of the mounting systems with tilt angle recommended by IDAE Technical Report, Lorenzo's equation, and Jacobson's equation. The parameters used for comparison are: photovoltaic field area gain, energy gain, and levelized cost of energy. The optimal photovoltaic module layout obtains the maximum photovoltaic field area gain of 35.52% with respect to the Jacobson's equation and the minimum of 32.29% with respect to the IDAE Technical Report. The optimal photovoltaic module layout obtains the maximum energy gain of 27.83% with respect to the Jacobson's equation and the minimum of 24.84% with respect to the IDAE Technical Report. The levelized cost of energy of the optimal PV module layout is lower than that of the other arrangements studied.

The algorithm presented may be useful by decision-makers or policymakers in determining the optimal distribution of photovoltaic modules on irregular rooftop shapes. Future work will consist of extending this study to different sites around the world to analyze the influence of site latitude. Another possible extension of the work would be to analyze the influence of the roof shape on the energy captured by the photovoltaic field. Moreover, the model could further be improved considering the shadowing produced by the building components.

Nomenclature

- A_{PV}^T Total PV modules area (m²)
- A_{PV}^E Effective PV modules area (m²)
- B Value of the shadow (m)
- C_{cb} Costs of the cable (€)
- C_i Initial investment cost (€)
- C_{inv} Unit cost of the inverter (€/unit)
- C_{MS} Unit cost of the mounting structure (€/unit)
- C_{OM} Cost of operation and maintenance (€)
- C_{pd} Costs of the protection devices (€)
- C_{PV} Unit cost of a PV module (€/unit)
- d Annual degradation rate
- EG Energy gain (%)
- E_a Total annual energy on the PV modules (MWh)
- E_{PV} Total energy on the PV modules (MWh)
- e_b Rooftop boundary distance (m)
- e'_b Building components boundary distance(m)
- e_l Longitudinal installation distance (m)
- e_l^m Longitudinal maintenance distance (m)
- e_l^{st} Longitudinal standard distance (m)
- e_t Transversal installation distance (m)
- h_R Lower limit of the integral

- h_S Upper limit of the integral
- \mathbb{I}_{bh} Adjusted beam irradiance on a horizontal surface (W/m²)
- \mathbb{I}_{dh} Adjusted diffuse irradiance on a horizontal surface (W/m²)
- \mathbb{I}_t Adjusted total irradiance on a tilted plane (W/m²)
- L Length of the mounting system (m)
- L_{BC} Length of the building components (m)
- L_R Length of the rectangle (m)
- L_{PV} Length of the PV module (m)
- $LCOE$ Levelized cost of electricity produced €/kWh)
- $LCOE$ efficiency Levelized cost of electricity produced efficiency
- N_{MS} Number of mounting systems
- N_{MSns} Number of mounting systems not shaded
- N_{PV} Number of PV modules
- n Ordinal of the day (day)
- $PVAG$ PV field area gain (%)
- \bar{P} Available rooftop area (m²)
- Q_i Availability of solar resource at the i th year (kWh)
- \bar{R} Rectangle where \bar{P} is inscribed (m²)
- S Projection the L on the horizontal plane (m)
- r Discount rate for i th year
- T Solar time (h)
- T_a Initial hour where cosine of incidence angle is positive (h)
- T_b Final hour where cosine of incidence angle is positive (h)
- T_R Sunrise solar time (h)
- T_S Sunset solar time (h)
- T_1 Initial hour where absence of shading is guaranteed(h)
- T_2 Final hour where absence of shading is guaranteed(h)
- W Width of the mounting system (m)
- W_{BC} Width of the building components (m)
- W_R Width of the rectangle (m)
- W_{PV} Width of the PV modules (m)
- α_S Height angle of the sun (°)
- β Tilt angle of PV module (°)
- β^* Tilt angle of PV module for the maximization of the total energy (°)
- γ Azimuth angle of PV module (°)
- γ_S Azimuth of the sun (°)
- δ Solar declination (°)
- θ_i Incidence angle (°)
- θ_l Longitudinal incidence angle (°)
- θ_{l0} Longitudinal incidence angle that minimizes shadowing effects (°)
- θ_z Zenith angle of the sun (°)
- λ Latitude angle (°)
- ρ_g Ground reflectance (dimensionless)
- ω Hour angle (°)

CRedit authorship contribution statement

A. Barbón: Conceptualization, Methodology. **M. Ghodbane:** Conceptualization, Methodology, Writing – original draft. **L. Bayón:** Software, Conceptualization, Methodology. **Z. Said:** Conceptualization, Methodology, Writing – original draft.

Declaration of competing interest

The authors declare that they have no known competing financial interests or personal relationships that could have appeared to influence the work reported in this paper.

References

- Al Garni, H.Z., Awasthi, A., Wright, D., 2019. Optimal orientation angles for maximizing energy yield for solar PV in Saudi Arabia. *Renew. Energy* 133, 538–550.
- Allouhi, A., Saadani, R., Buker, M.S., Kousksou, T., Jamil, A., Rahmoune, M., 2019. Energetic, economic and environmental (3E) analyses and LCOE estimation of three technologies of PV grid-connected systems under different climates. *Sol. Energy* 178, 25–36.
- Ascencio-Vásquez, J., Brecl, K., Topič, M., 2019. Methodology of Köppen-Geiger-Photovoltaic climate classification and implications to worldwide mapping of PV system performance. *Sol. Energy* 191, 672–685.
- Autosolar, 2021. Technical data. Available from: <https://autosolar.es/>. Accessed 26 April 2022.
- Bahrami, A., Okoye, C.O., Atikol, U., 2017. Technical and economic assessment of fixed, single and dual-axis tracking PV panels in low latitude countries. *Renew. Energy* 113, 563–579.
- Barbón, A., Bayón-Cueli, C., Bayón, L., Rodríguez-Suanzes, C., 2022. Analysis of the tilt and azimuth angles of photovoltaic systems in non-ideal positions for urban applications. *Appl. Energy* 305, 117802.
- Barbón, A., Fortuny Ayuso, P., Bayón, L., Fernández-Rubiera, J.A., 2020. Predicting beam and diffuse horizontal irradiance using Fourier expansions. *Renew. Energy* 154, 46–57.
- Barbón, A., Fortuny Ayuso, P., Bayón, L., Silva, C.A., 2021. A comparative study between racking systems for photovoltaic power systems. *Renew. Energy* 180, 424–437.
- Bayón-Cueli, C., Barbón, A., Fernández-Conde, A., Bayón, L., 2021. Optimal distribution of PV modules on roofs with limited space. In: *IEEE International Conference on Environment and Electrical Engineering*. pp. 1–6.
- Belsky, A.A., Glukhanich, D.Y., Carrizosa, M.J., Starshaia, V.V., 2022. Analysis of specifications of solar photovoltaic panels. *Renew. Sustain. Energy Rev.* 159, 112239.
- Bey, M., Hamidat, A., Nacer, T., 2021. Eco-energetic feasibility study of using grid-connected photovoltaic system in wastewater treatment plant. *Energy* 216, 119217.
- Brecl, K., Topič, M., 2011. Self-shading losses of fixed free-standing PV arrays. *Renew. Energy* 36, 3211–3216.
- British Petroleum, 2021. *Statistical Review of World Energy*, 70th ed. <https://www.bp.com/content/dam/bp/business-sites/en/global/corporate/pdfs/energy-economics/statistical-review/bp-stats-review-2021-full-report.pdf>. Accessed 23 March 2022.
- Byrne, J., Taminiau, J., Kurdgelashvili, L., Nam Kim, K., 2015. A review of the solar city concept and methods to assess rooftop solar electric potential, with an illustrative application to the city of Seoul. *Renew. Sustain. Energy Rev.* 41, 830–844.
- Chinchilla, M., Santos-Martín, D., Carpintero-Rentería, M., Lemon, S., 2021. Worldwide annual optimum tilt angle model for solar collectors and photovoltaic systems in the absence of site meteorological data. *Appl. Energy* 281, 116056.
- Conceição, R., Silva, H.G., Fialho, L., Lopes, F.M., Collares-Pereira, M., 2019. PV system design with the effect of soiling on the optimum tilt angle. *Renew. Energy* 133, 787–796.
- Dehwal, A.H.A., Asif, M., Rahman, M.T., 2018. Prospects of PV application in unregulated building rooftops in developing countries: A perspective from Saudi Arabia. *Energy Build.* 171, 76–87.
- Duffie, J.A., Beckman, W.A., 2013. *Solar Engineering of Thermal Processes*. John Wiley & Sons.
- European Union, 2009. Directive 2009/28/EC, on the promotion of the use of energy from renewable sources.
- European Commission, 2014. A policy framework for climate and energy in the period from 2020 to 2030.
- European Union, 2018. Directive 2018/2001/EC, on the promotion of the use of energy from renewable sources.
- Fernández-Infantes, A., Contreras, J., Bernal-Agustín, J.L., 2006. Design of grid connected PV systems considering electrical, economical and environmental aspects: A practical case. *Renew. Energy* 31, 2042–2062.
- Gernaat, D.E.H.J., Sytze de Boer, H., Dammeier, L.C., van Vuuren, D.P., 2020. The role of residential rooftop photovoltaic in long-term energy and climate scenarios. *Appl. Energy* 279, 115705.
- Ghodbane, M., Boumeddane, B., Said, Z., Bellos, E., 2019. A numerical simulation of a linear Fresnel solar reflector directed to produce steam for the power plant. *J. Cleaner Prod.* 231, 494–508.
- Giffith, B., Torcellini, P., Long, N., 2006. Assessment of the technical potential for achieving zero-energy commercial buildings. In: *Proceedings of the ACEEE Summer Study Pacific Grove*.
- Hachem, C., Athienitis, A., Fazio, P., 2011. Investigation of solar potential of housing units in different neighborhood designs. *Energy Build.* 43 (9), 2262–2273.
- Institute for Energy Diversification and Saving, 2002. Technical Conditions for PV Installations Connected to the Grid [in Spanish]. Spanish Government Technical Report, <http://www.idae.es>, 2002. Accessed 10 September 2021.
- Institute for Energy Diversification and Saving, 2011. Technical Conditions for PV Installations Connected to the Grid [in Spanish]. Spanish Government Technical Report, <http://www.idae.es>. Accessed 4 March 2022.
- International Renewable Energy Agency, 2019. Trends in photovoltaic applications 2019. <https://iea-pvps.org/publications/technical-reports/>. Accessed 14 March 2022.
- Iliopoulos, T.G., Fermeleglia, M., Vanheusden, B., 2020. The EU's 2030 climate and energy policy framework: How net metering slips through its net. *Rev. Eur. Comp. Int. Environ. Law* 29, 245–256.
- Imahori, S., Yagiura, M., Nagamochi, H., 2006. *Practical Algorithms for Two-Dimensional Packing*. Department of mathematical informatics, University of Tokyo, METR2006-19.
- Ioannou, A.K., Stefanakis, N.E., Boudouvis, A.G., 2014. Design optimization of residential grid-connected photovoltaics on rooftops. *Energy Build.* 76, 588–596.
- International Renewable Energy Agency, 2017. Solar costs to fall further, powering global demand. <https://www.reuters.com/article/singapore-energy-solar-idUSL4N1MY2F8>. Accessed 14 March 2022.
- International Renewable Energy Agency, 2019. Future of solar photovoltaic: deployment, investment, technology, grid integration and socio-economic aspects. https://irena.org/-/media/Files/IRENA/Agency/Publication/2019/Nov/IRENA_Future_of_Solar_PV_2019.pdf. Accessed 23 December 2021.
- Jacobson, M.Z., Delucchi, M.A., Bauer, Z.A.F., Goodman, S.C., Chapman, W.E., Cameron, M.A., Bozonnat, C., Chobadi, L., Clonts, H.A., Enevoldsen, P., Erwin, J.R., Fobi, S.N., Goldstrom, O.K., Hennessy, E.M., Liu, J., Lo, J., Meyer, C.B., Morris, S.B., Moy, K.R., O'Neill, P.L., Petkov, I., Redfern, S., Schucker, R., Sontag, M.A., Wang, J., Weiner, E., Yachanin, A.S., 2017. 100% Clean and renewable wind, water, and sunlight (WWS) all-sector energy roadmaps for 139 countries of the world. *Joule* 1, 108–121, (Alphabetical).
- Jacobson, M.Z., Jadhav, V., 2018. World estimates of PV optimal tilt angles and ratios of sunlight incident upon tilted and tracked PV panels relative to horizontal panels. *Sol. Energy* 169, 55–66.
- Jafarkazemi, F., Saadabadi, S.A., 2013. Optimum tilt angle and orientation of solar surfaces in Abu Dhabi, UAE. *Renew. Energy* 56, 44–49.
- Jallal, M.A., El Yassini, A., Chabaa, S., Zeroual, A., Ibyaich, S., 2020. Ensemble learning algorithm-based artificial neural network for predicting solar radiation data. In: *IEEE International Conference on Decision Aid Sciences and Application (DASA)*. pp. 526–531.
- Jurasz, J.K., Dabek, P.B., Campana, P.E., 2020. Can a city reach energy self-sufficiency by means of rooftop photovoltaics? Case study from Poland. *J. Cleaner Prod.* 245, 118813.
- Khalil Zidane, T.E., Bin Adzman, M.R., Naim Tajuddin, M.F., Mat Zali, S., Durusu, A., 2019. Optimal configuration of photovoltaic power plant using grey wolf optimizer: A comparative analysis considering CdTe and c-Si PV modules. *Sol. Energy* 188, 247–257.
- Korsavi, S.S., Zomorodian, Z.S., Tahsildoost, M., 2018. Energy and economic performance of rooftop PV panels in the hot and dry climate of Iran. *J. Cleaner Prod.* 174, 1204–1214.
- Lang, T., Gloerfeld, E., Girod, B., 2015. Don't just follow the sun—A global assessment of economic performance for residential building photovoltaics. *Renew. Sustain. Energy Rev.* 42, 932–951.
- Lau, K.Y., Tan, C.W., Ching, K.Y., 2021. The implementation of grid-connected, residential rooftop photovoltaic systems under different load scenarios in Malaysia. *J. Cleaner Prod.* 316, 128389.
- Liu, B.Y.H., Jordan, R.C., 1963. The long-term average performance of flat-plate solar energy collectors. *Sol. Energy* 7, 53–74.
- Lorenzo, E., 2011. Energy collected and delivered by PV modules. In: *Handbook of Photovoltaic Science and Engineering*. John Wiley & Sons, New Jersey, pp. 984–1042.
- Makhdoomi, S., Askarzadeh, A., 2021. Impact of solar tracker and energy storage system on sizing of hybrid energy systems: A comparison between diesel/PV/PHS and diesel/PV/FC. *Energy* 231, 120920.
- Mamun, M.A.A., Islam, M.M., Hasanuzzaman, M., Selvaraj, J., 2021. Effect of tilt angle on the performance and electrical parameters of a PV module: Comparative indoor and outdoor experimental investigation. *Energy Built Environ.* 3 (3), 278–290.

- Marzo, A., Ferrada, P., Beiza, F., Besson, P., Alonso-Montesinos, J., Ballestrín, J., Román, R., Portillo, C., Escobar, R., Fuentealba, E., 2018. Standard or local solar spectrum? Implications for solar technologiessudies in the Atacama desert. *Renew. Energy* 127, 871–882.
- Melius, J., Margolis, R., Ong, S., 2013. Estimating Rooftop Suitability for PV: A Review of Methods, Patents, and Validation Techniques. National Renewable Energy Laboratory (NREL), pp. 1–30.
- Mousazadeh, H., Keyhani, A., Javadi, A., Mobli, H., 2009. A review of principle and sun-tracking methods for maximizing solar systems output. *Renew. Sustain. Energy Rev.* 13, 1800–1818.
- National Geographic Information Centre of the Government of Spain, 2022. <http://centrodedescargas.cnig.es/CentroDescargas/> Accessed 1 March 2022.
- Nicolás-Martín, C., Santos-Martín, D., Chinchilla-Sánchez, M., Lemon, S., 2020. A global annual optimum tilt angle model for photovoltaic generation to use in the absence of local meteorological data. *Renew. Energy* 161, 722–735.
- National Renewable Energy Laboratory, 2018. Best Practices for Operation and Maintenance of Photovoltaic and Energy Storage Systems, third ed. Golden, CO, <https://www.nrel.gov/docs/fy19osti/73822.pdf>. Accessed 1 March 2022.
- Odyssee-Mure, 2015. Energy efficiency trends in buildings in the EU lessons from the ODYSSEE MURE project. <http://www.odyssee-mure.eu/publications/br/energy-efficiency-trends-policies-buildings.pdf>. Accessed 6 March 2022.
- Park, S., Nielsen, A., Bailey, R.T., Trolle, D., Bieger, K., 2019. A QGIS-based graphical user interface for application and evaluation of SWAT-MODFLOW models. *Environ. Model. Softw.* 111, 493–497.
- PVGIS, Joint Research Centre (JRC), 2022. <https://ec.europa.eu/jrc/en/pvgis>.
- Said, Z., Ghodbane, M., Boumeddane, B., Tiwari, A.K., Sundar, L.S., Li, C., Aslfattahi, N., Bellos, E., 2022. Energy, exergy, economic and environmental (4E) analysis of a parabolic trough solar collector using MXene based silicone oil nanofluids. *Sol. Energy Mater. Sol. Cells* 239, 111633.
- Sebbah, B., Yazidi Alaoui, O., Wahbi, M., Maâtouk, M., Ben Achhab, N., 2021. QGIS-Landsat Indices plugin (Q-LIP): Tool for environmental indices computing using Landsat data. *Environ. Model. Softw.* 137, 104972.
- Siraki, A.G., Pillay, P., 2012. Study of optimum tilt angles for solar panels in different latitudes for urban applications. *Sol. Energy* 86, 1920–1928.
- Talavera, D.L., Muñoz-Cerón, E., Ferrer-Rodríguez, J.P., Pérez-Higueras, P.J., 2019. Assessment of cost-competitiveness and profitability of fixed and tracking photovoltaic systems: the case of five specific sites. *Renew. Energy* 134, 902–913.
- Tibebu, T.B., Hittinger, E., Miao, Q., Williams, E., 2021. What is the optimal subsidy for residential solar? *Energy Policy* 155, 112326.
- Tröndle, T., Pfenninger, S., Lilliestam, J., 2019. Home-made or imported: On the possibility for renewable electricity autarky on all scales in Europe. *Energy Strategy Rev.* 26, 100388.
- Wang, M., Mao, X., Gao, Y., He, F., 2018. Potential of carbon emission reduction and financial feasibility of urban rooftop photovoltaic power generation in Beijing. *J. Cleaner Prod.* 203, 1119–1131.
- Yadav, A.S., Mukherjee, V., 2021. Conventional and advanced PV array configurations to extract maximum power under partial shading conditions: A review. *Renew. Energy* 178, 977–1005.